

**Chemical syntheses of the salvinorin chemotype of KOR  
agonist**

Journal:	<i>Natural Product Reports</i>
Manuscript ID	NP-HIG-05-2020-000028.R1
Article Type:	Review Article
Date Submitted by the Author:	21-Jul-2020
Complete List of Authors:	Hill, Sarah; Scripps Research Institute, Chemistry Brion, Aurélien; Université Paris Sciences et Lettres Shenvi, Ryan; Scripps Research Institute, Chemistry

## Chemical Syntheses of the salvinorin chemotype of KOR agonist

Sarah J. Hill, Aurélien U. C. M. Brion, Ryan A. Shenvi\*

Department of Chemistry, The Scripps Research Institute, 10550 North Torrey Pines Road, La Jolla, California 92037, United States

**Abstract.** The hallucinogenic diterpene salvinorin A potently and selectively agonizes the human  $\kappa$ -opioid receptor (KOR). Its unique attributes—lack of a basic nitrogen, rapid brain penetrance, short half-life—combined with the potential of KOR as an emerging target for analgesics have stimulated extensive medicinal chemistry based on semi-synthesis from extracts of *Salvia divinorum*. Total synthesis efforts have delivered multiple, orthogonal routes to salvinorin A, its congeners and related analogs with the goal of optimizing its activity towards multiple functional endpoints. Here we review total syntheses of the salvinorin chemotype and discuss outstanding problems that synthesis can address in the future.

## 1. Introduction

## 2. Rook and Perlmutter Approaches

## 3. Evans' Asymmetric Synthesis

## 4. Hagiwara's Asymmetric First Generation Synthesis

## 5. Hagiwara's Asymmetric Second Generation Synthesis

## 6. Hagiwara's Salvinorin F Synthesis

## 7. Forsyth's Asymmetric Synthesis

## 8. Metz's Synthesis

## 9. Prisinzano's Analog Total Synthesis

## 10. Shenvi's 20-nor-SalA and O6C-Sal Synthesis

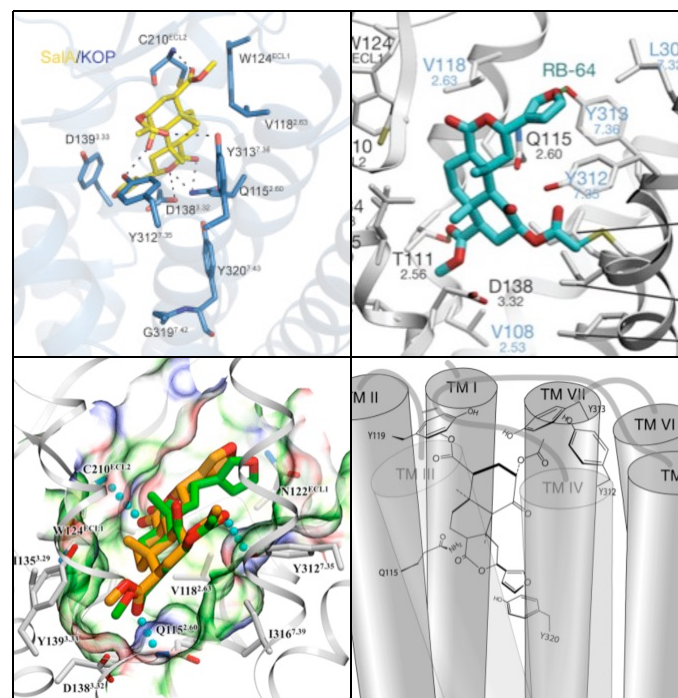
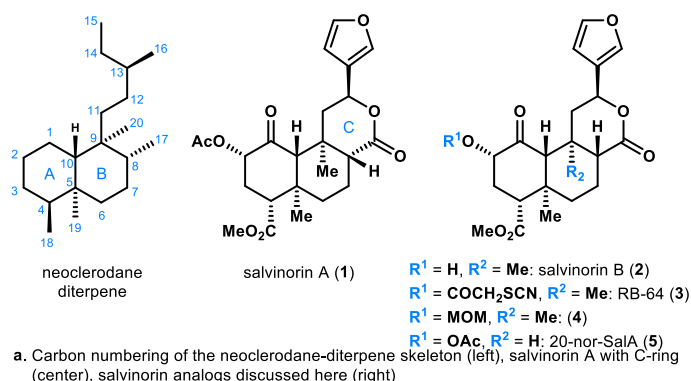
## 11. Route Comparisons

## 12. Scaffold Hopping versus Dynamic Retrosynthesis

## 13. Conclusion

1. Introduction

Opioid addiction and overdose have been rising problems in the United States and around the world since the late 1990s when prescriptions of opioids to treat chronic pain began to increase sharply.<sup>1</sup> In 2017, 1.7 million Americans abused prescription opioids or related substances; 2018 saw 128 deaths per day from opioid overdose.<sup>2,3</sup> Humans express four types of opioid receptors:  $\mu$ ,  $\kappa$ ,  $\delta$ , and the nociceptin receptor. All are G protein-coupled receptors (GPCRs) associated with the  $G_i$  protein, meaning each inhibit adenylyl cyclase upon activation, which produces an analgesic effect, pain relief.<sup>4</sup> Many prescription opioids associated with addiction, overdose and death (e.g. morphine, oxycodone, codeine, fentanyl) are agonists of the  $\mu$ -opioid receptor.<sup>5</sup> This receptor is implicated in physical dependence and respiratory depression side-effects more than its related family member, the  $\kappa$ -opioid receptor (KOR).<sup>6</sup> Pharmacology of the  $\kappa$ -opioid receptor is challenging and underexplored, making selective ligands of the  $\kappa$ -opioid receptor valuable targets. Like many



b.  $\kappa$ -opioid receptor (KOR) binding proposals. *Top left*: salvinorin A docked in nanobody stabilized active state KOR [Ref. 8]; *top right*: RB 64 docked in crystal structure of KOR [Ref. 56]; covalently attached to C-315; *bottom left*: 20-nor-SalA docked in KOR [Ref. 17]; *bottom right*: SalA docked in KOR showing transmembrane (TM) loops [Ref. 70]

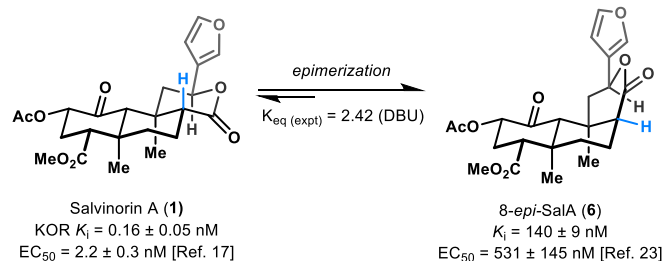


Figure 1. Salvinorin diterpenes and select analogues.

GPCRs, KORs exist in a dynamic state, changing from inactive to multiple active conformations of varying stability upon agonist binding.<sup>7</sup> Recently, an active-state crystal structure of the  $\kappa$ -opioid receptor has been solved,<sup>8</sup> but its many related active conformations and the structural effects of small molecule ligands remain uncertain.

The multiple active conformations of the KOR provide the basis for ligands to bias signaling pathways. Both G-protein dependent and independent signaling can occur when an agonist binds. Whereas the G-protein dependent pathway inhibits adenylyl cyclase activity and regulates cAMP levels, the G-protein independent pathway activates MAP kinases which recruit  $\beta$ -arrestin proteins and ultimately internalize the receptor.<sup>9</sup> Research suggests that negative side effects associated with KOR activation, such as dysphoria and psychotomimesis,<sup>10</sup> are caused by activation of  $\beta$ -arrestin, whereas useful analgesic effects are linked to the G-protein dependent pathway. Bohn demonstrated in 2016 that triazole agonists of the KOR biased for the G-protein dependent pathway relieved pain and itch in mice without reductions in locomotion or dopamine levels, effects associated with dysphoria.<sup>11</sup> Other studies have shown that mutant KORs which are not phosphorylated by GRKs (G-protein coupled receptors kinases) do not induce condition place aversion,<sup>12</sup> while antinociception is maintained in  $\beta$ -arrestin knock out mice.<sup>13</sup> The exact consequence of this divergent signaling is not settled science and still sparks debate, as represented by claims that  $\beta$ -arrestin signaling was not needed for KOR agonist-mediated aversion.<sup>14</sup> Many unanswered questions regarding biased ligand pharmacology have driven researchers to explore new and unique KOR agonists.

The salvinorin class of neoclerodane diterpenoid (**Figure 1**) was first isolated from *Salvia divinorum*, a plant found in Southern Mexico.<sup>15</sup> Salvinorin A (SaLA) (**1**, **Figure 1**) was identified as the main hallucinogenic component of *S. divinorum* and annotated as a potent and selective  $\kappa$ -opioid receptor agonist.<sup>16</sup> It is unique among opioid receptor ligands in its lack of nitrogen atoms but high affinity ( $K_i = 160$  pM) for KOR.<sup>17</sup> Basic amines in opioid ligands were previously thought necessary for high affinity binding via formation of a salt-bridge with a conserved aspartate residue.<sup>18, 19</sup> Many conflicted docked poses of SaLA in the KOR have been proposed in the literature (**Figure 1b**). The unusual, unknown binding mode and high selectivity for KOR have stimulated many SaLA analogue and bioassay campaigns. The overwhelming majority of these analogues were produced through semi-synthesis, and changes were generally limited to substitutions at the C2 acetate, C4 ester, and C12 furan. An extensive body of literature and several reviews have compared SaLA analogue affinities and potencies ( $EC_{50}$ ) of KOR binding and activation.<sup>20</sup> While most analogues exhibited lower potency compared to SaLA, some have improved activity or favorable properties: a methoxy methyl ether substitution at C2 improved the  $EC_{50}$  and replaced the metabolically labile acetate.<sup>21</sup> Some analogues have even shown biased agonism through an isothiocyanate substitution at C2.<sup>22</sup>

Two problems impede structure activity relationship (SAR) studies of SaLA. The first involves scaffold instability, as SaLA undergoes epimerization at C8 to its significantly less potent isomer in mildly basic conditions (**Figure 1c**);<sup>23, 24</sup> bioassays of mixtures of epimers could produce inconclusive or conflicting results. The second hinderance is the synthetic challenge posed by SaLA. The highly

oxidized all *trans*-fused 6/6/6 ring system and its seven stereocenters present an obstacle daunting enough to prompt greater than 40 semi-synthesis campaigns. Intriguing biological profiles combined with synthetic complexity have suggested SaLA and its congeners as important targets for total synthesis investigation. Several groups have sought a solution practical enough to enable a medicinal chemistry campaign. This review will cover the approaches towards and completed total syntheses of SaLA and other related salvinorin scaffolds. Their benefits and deficits will be highlighted and put into the larger context of continued exploration of SaLA SAR and the capability to further elucidate KOR pharmacology.

## 2. Rook and Perlmutter Approaches

The first attempt to synthesize SaLA was made in 2006 by Rook and coworkers (**Figure 2**).<sup>25</sup> Their analysis of the scaffold suggested that retrosynthetic disconnection of the natural product into two relatively equal sized halves, an A-ring cyclohexanone **7** and C-ring  $\delta$ -lactone **10**, would offer some benefit to synthesis: efficiency and convergency. Conversion of these two fragments to SaLA, although never attempted, was proposed to be feasible by Michael addition, followed by ring-closing olefin metathesis and hydrogenation.

Initial attempts to enantioselectively synthesize A ring fragment **7** relied on pseudoephedrine as a chiral auxiliary to effect a diastereoselective Diels-Alder reaction between methyl acrylate **9** and complex furan **8**. This building block was accessed from enyne **11** via condensation with (+)-pseudoephedrine to produce enamine **12**, followed by acidic deprotection and base-induced cyclization to furan **13**, another acidic deprotection yielded desired furan **8**. Alternative use of (-)-ephedrine provided access to the diastereomer of **14**. Surprisingly, both series of auxiliary led to the same enantiomeric series of cycloadduct but in different diastereomeric ratios.

Treatment of **8** with methyl acrylate and water, followed by hydrolysis with buffered acetic acid produced a 1:1 mixture of **15** and **16** derived from exo and endo Diels-Alder cycloadducts, whereas stereoisomer **14** led to a 1:9 ratio. Unfortunately, exo isomer **15** embodied the correct relative stereochemistry at C2 and C4, so absence of selectivity actually provided the highest throughput and yielded **15** in moderate enantiomeric excess (60% *ee*). Treatment of **15** with boron tribromide followed by quench with 2,4,6-collidine furnished cyclic enone **17**; relative stereochemistry was confirmed by observation of a NOE enhancements between the C2 and C4 protons, which were absent in the ring opened endo adduct. Acetylation of enone **17** was accomplished by acetyl chloride in the collidine-quenched solution of the boron tribromide reaction. All attempts to isolate **17** or acetylated **18** by normal phase chromatography led to epimerization at C4. Although reverse phase HPLC suppressed epimerization, this sequence was only attempted on *rac*-**15**; salemic **18** was never produced and the planned conjugate addition of a vinyl organometallic was not reported.

The Perlmutter group also published an approach towards the salvinorin A scaffold (**Figure 3**) and planned to probe the biological consequences of C20 removal.<sup>26</sup> In contrast to later work,<sup>17</sup> this study did not associate the C20 methyl with SaLA scaffold destabilization or recognize its effects on C8 epimerization. Instead, its importance was attributed to its absence from semi-synthetic SAR studies. Like Rook,

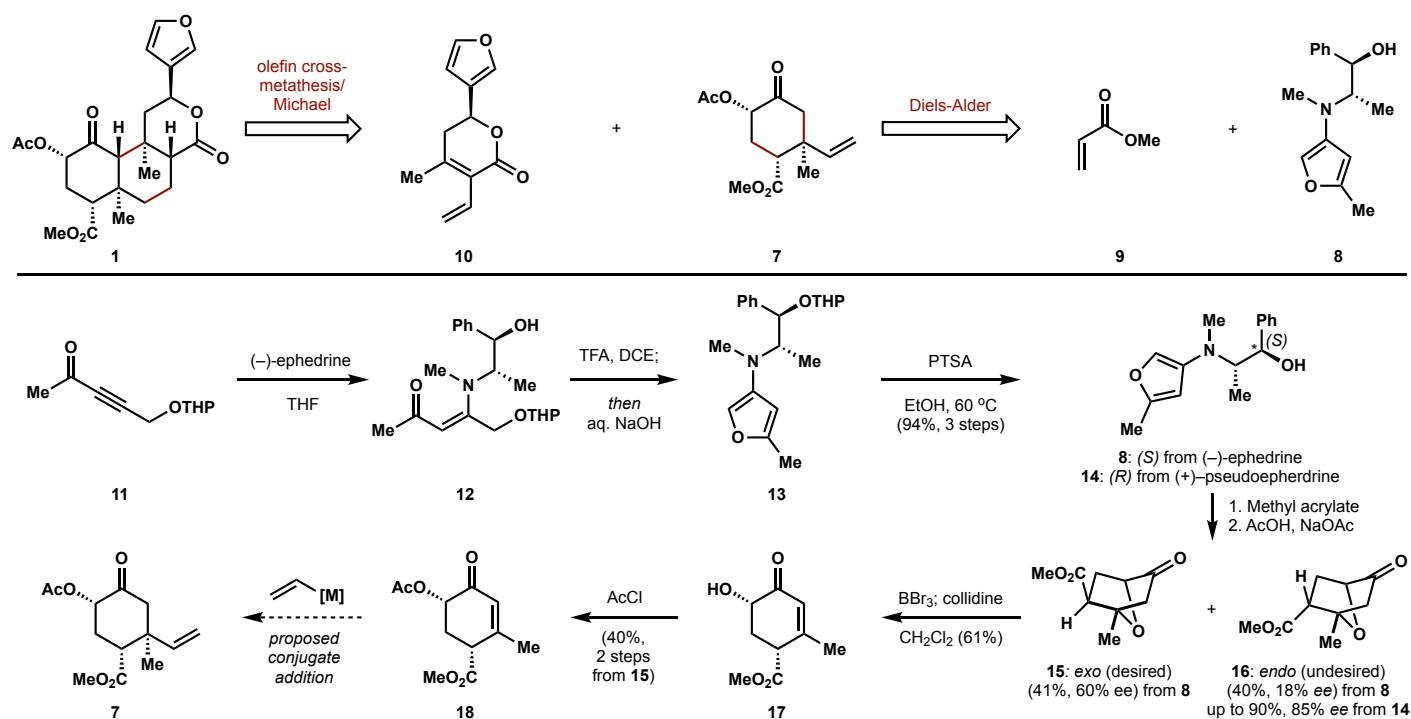


**Figure 2.** Rook's approach to the A-ring of salvinorin A illustrated the difficulty of these substituted building blocks.

the synthesis design relied on a key Diels-Alder cycloaddition, in this case between a quinone surrogate of the A-ring and a dienyl C-ring. This diene reaction partner **20** had previously been synthesized via enyne metathesis by Snapper in syntheses of the cacospongionolide sesterterpenes.<sup>27</sup> Reaction with quinone **22** and  $\text{TiCl}_4$  delivered Diels-Alder adduct **23** in a modest 37% yield but with several key stereocenters formed in high selectivity. C10 was then epimerized by DBU to generate tricycle **24** with a surprising *trans*-A/B enedione ring junction and all skeletal carbons in place. Conjugate reduction was effected by sodium dithionite ( $\text{Na}_2\text{S}_2\text{O}_4$ ) in toluene/ $\text{H}_2\text{O}$  containing Adogen 464, a long-chain alkylammonium chloride, to give tricycle **19**, the furthest advanced intermediate achieved.

Perlmutter's approach rapidly assembled the tricyclic Sala core with the correct stereochemistry of key non-epimerizable stereocenters. Although conjugate reduction conditions were identified to bring the A-ring closer to the correct oxidation state, these intermediates were not elaborated further towards Sala or 20-nor-Sala. A later variation on Perlmutter's approach was published by Hanquet in 2011 that used the same dienophile appended with a chiral sulfoxide to couple with racemates of the dienes.<sup>28</sup> These two approaches showcase the deceptive simplicity of the salvinorin scaffold, especially when a robust, practical synthetic approach must be achieved. Several total syntheses of Sala have chased this elusive goal, but the target itself may represent a red-herring.

### 3. Evans' Asymmetric Synthesis

The first total synthesis of Sala was accomplished by the Evans group in 2007: a 29-step, asymmetric route that featured an unusual transannular Michael cascade from a macrocyclic lactone

(**Figure 4**).<sup>29</sup> This approach took inspiration from Evans' prior work on FR182877 and hexacyclinic acid, which involved transannular Diels-Alder cycloadditions to forge multiple stereocenters of a fused polycycle.<sup>30</sup> Although macrocyclic subtargets are normally deprioritized in retrosynthetic analysis, macrocyclic stereocontrol combined with downstream synthetic ease can influence risk assessment. Macrolactones, in particular, can be especially easy to synthesize. Macrolactone **25** and its acyclic precursor **37** can be traced back via fragment coupling to a vinyl iodide furanyl segment **26** and functionalized aldehyde **27**.

Synthesis of the aldehyde fragment began with an enantioselective, nickel catalyzed ortho-ester alkylation, followed by a Claisen condensation to yield  $\beta$ -keto ester **29** in high enantioselectivity and yield. Phosphorylation and subsequent cross coupling installed the C19 methyl group with selectivity for the *E*-stereoisomer derived from (*Z*)-enol phosphate geometry. The  $\alpha,\beta$ -unsaturated ester was converted to the aldehyde via reduction/oxidation, and engaged in an asymmetric aldol reaction controlled by an Evans auxiliary. Auxiliary methanolysis, alkene oxidative cleavage and ephedrine-mediated asymmetric zinc acetylide addition provided **32**, which was advanced to aldehyde fragment **27** in three steps. Vinyl iodide **26** was synthesized from ynone **33** via asymmetric reduction and alkyne isomerization, followed by carboalumination/iodination and alcohol protection as the triethylsilyl ether.

Fragment coupling was achieved by conversion of vinyl iodide **26** into its Grignard reagent via lithium-halogen exchange and transmetalation by magnesium bromide etherate; diastereoselective addition to aldehyde **27** was governed by chelation control by the neighboring BOM ether. Protecting group manipulations and



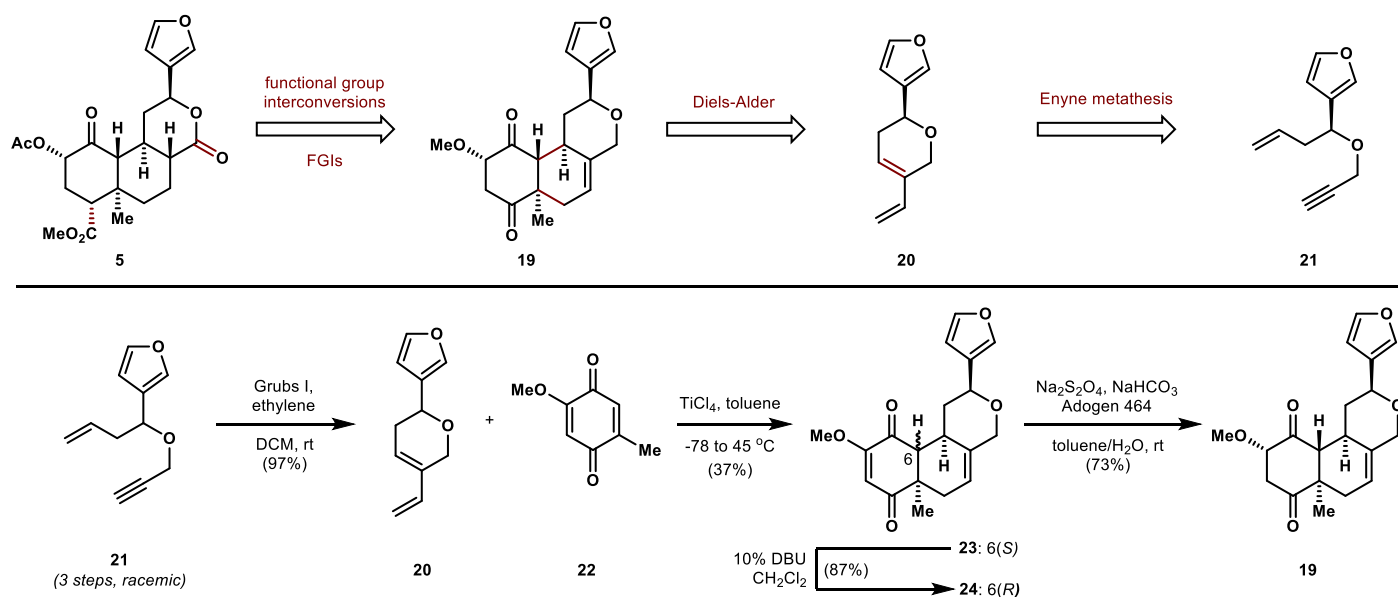


**Figure 3.** Perlmutter established a remarkably concise 7-step approach to the salvinorin framework.

hydrolysis of the methyl ester furnished macrolactonization substrate **37**, which was cyclized as its mixed anhydride at high dilution (1.5 mM).<sup>31</sup> Addition of TBAF at  $-78\text{ }^{\circ}\text{C}$  initiated the transannular Michael cascade and delivered a single diastereomer **25**, having set three stereocenters, two quaternary. The authors rationalized the selectivity by a chair-like transition state that positions the bulkiest substituents in pseudo-equatorial positions and favor the *trans*-decalin ring junction. The final manipulations en route to SaIA include iterative reduction of the C7 ketone, which unfortunately almost completely favors the incorrect C8 stereoisomer **40**. Later treatment of **40** with methanolic potassium carbonate establishes an equilibrium with the correct stereoisomer **2** (salvinorin B) as the minor component (2.5:1). Acetylation of the C2 alcohol completes their synthesis of SaIA in 29 steps in 1% overall yield.

The Evans synthesis established a benchmark to measure subsequent SaIA syntheses. The transannular Michael cascade, while unconventional, forms quaternary stereocenters that are difficult to obtain in future efforts and establishes each of the seven stereocenters with absolute stereocontrol. If use as a blue-print for medicinal chemistry is the ultimate goal, the efficiency of this route must improve. The authors highlight control of C8 stereochemistry: the incorrect epimer was favored kinetically by *tert*-butanol protonation of the corresponding enolate and Munro *et al.* established that the same incorrect epimer is favored thermodynamically.<sup>32</sup> This feature creates a bottleneck in the synthesis, but also raises the specter of scaffold suitability: perhaps SaIA is a poor target for total synthesis.

#### 4. Hagiwara's First Generation Asymmetric Synthesis

The next total synthesis of SaIA was published by the Hagiwara group and also completed in an asymmetric fashion (**Figure 5**).<sup>33</sup> The Hagiwara strategy differs significantly from Evans in its orthodoxy, utilizing the reliable Wieland-Miescher ketone strategy to access neoclerodane terpenes.<sup>34,35</sup> While this approach avoids a macrocyclic

intermediate and begins with two rings already intact, the oxygenation pattern must be shifted by one position at multiple carbons—occasionally a challenging tactic. Some efficiency is gained back by parallel installation and oxidation of the C17 and C18 carbonyls.

The Wieland-Miescher ketone derivative **45**, synthesized in 3 steps in their previously reported synthesis of (-)-methyl barbascoate,<sup>34</sup> already possesses the A, B ring systems and C1 oxygen—an advanced starting point. Reductive alkylation with  $\alpha$ -iodo ethyl acetate furnished ketoester **47** in 51% yield, although significant material was lost due to alcohol elimination. Next, ketal removal followed by dual methylenation installed the C17 and C18 carbons concurrently. Further functional group manipulations arrived at intermediate **44**, which could be subjected to dual hydroboration/oxidation to the aldehydes of C17 and C18 in a high yielding sequence that formed both the C4 and C8 stereocenters with the desired stereochemistry after epimerization. Ketalization of the newly formed aldehydes followed by TBS removal and subsequent primary alcohol oxidation delivered a precursor to addition of the furan motif. Treatment of **53** with 3-lithiofuran at low temperature delivered alcohol **54** in useful yields but with low dr: 2:3 in favor of the incorrect diastereomer. These isomers, however, proved separable, and the target isomer could be subjected to acid-catalyzed deketalization to form lactol **55**. Oxidative hydrolysis with DDQ removed the MPM protecting group, and all that remained was to increase the oxidation states at C1, C2, C4, and C17. Three of these oxidations were accomplished in a single step with PDC; subsequent methyl ester formation furnished intermediate **43**, only missing the oxidation at C2. Rubottom oxidation was employed to accomplish this final transformation: formation of the C2 enol ether and oxidation with *m*-CPBA gave a 70% overall yield of the C2 C–O bond, but with the incorrect stereochemistry. A final Mitsunobu reaction inverted this stereocenter with concomitant incorporation of the target acetate, but required long duration and excess of reagents. As later noted by our group, Hagiwara acknowledges that this C2 acetylation is a

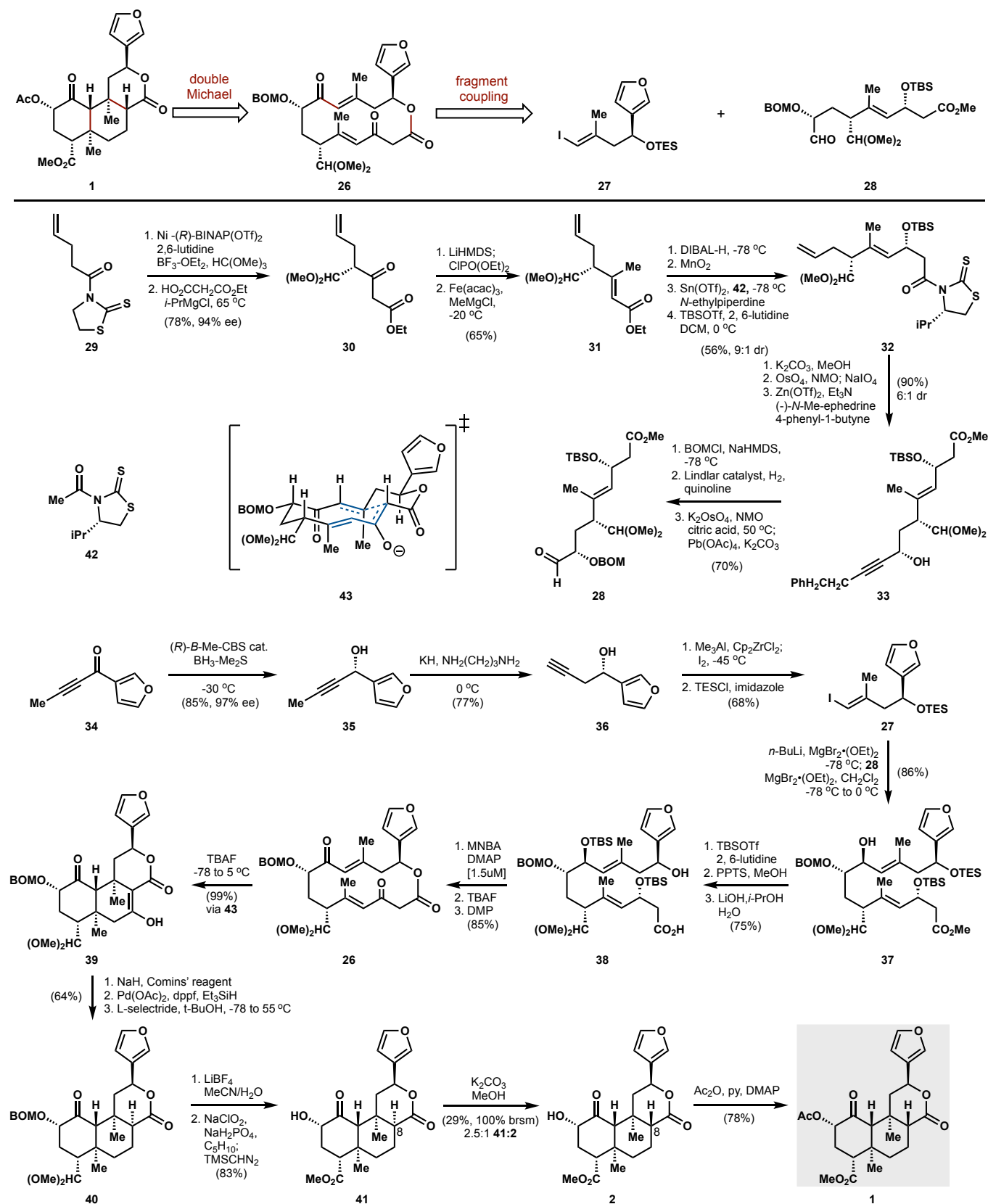


**Figure 4.** Evans' synthesis featured an unorthodox transannular Michael cascade to access the tricyclic core.

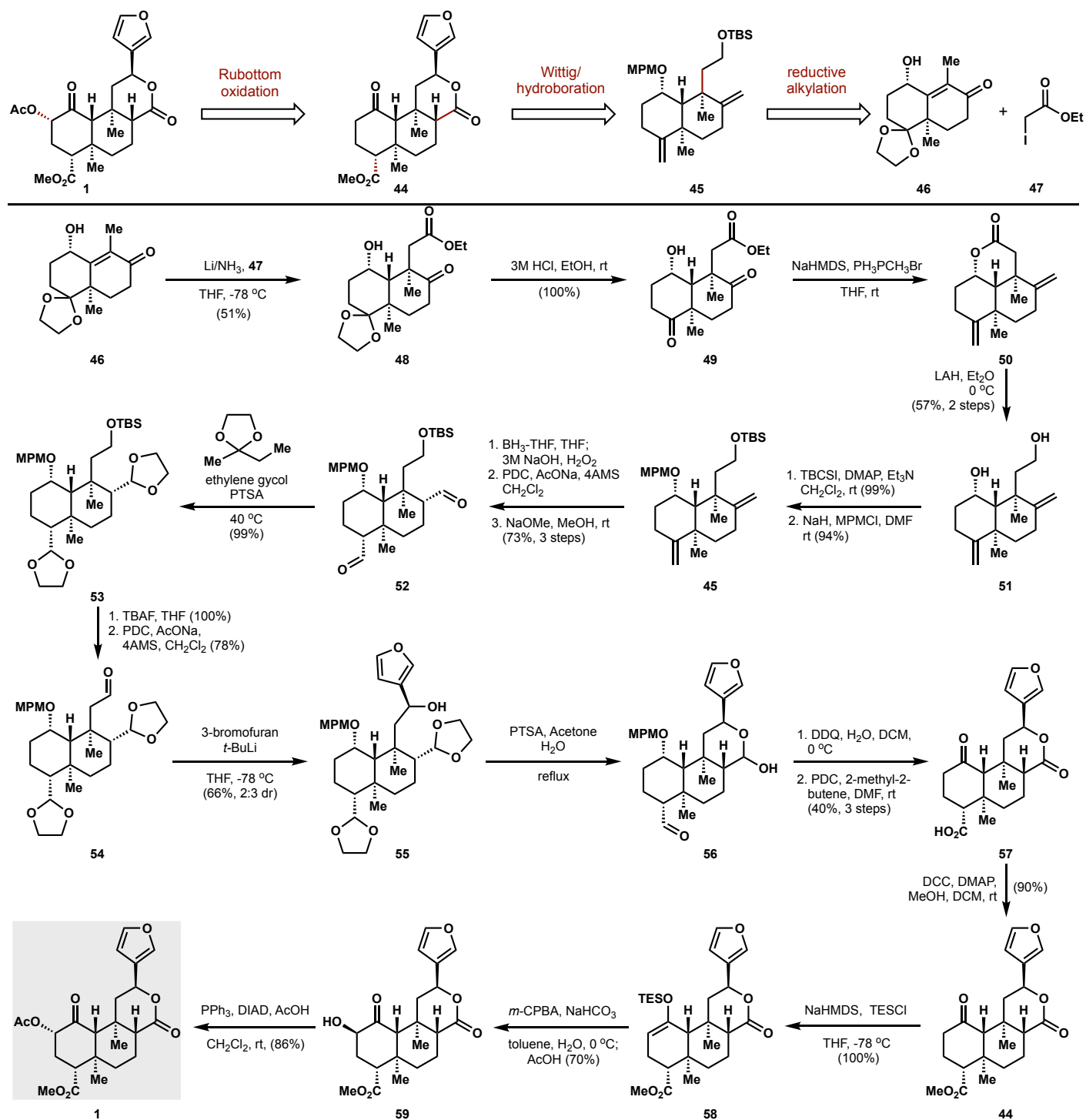


**Figure 5.** Hagiwara's first generation synthesis started from a Wieland-Miescher ketone derivative.

difficult task: competing epimerization and elimination decrease the yield, as does purification of excess reagent. This foundational work by the Hagiwara group constituted an efficient asymmetric synthesis of SalA in 20 steps and 0.5% overall yield. Most notably, the one-carbon

movement of oxidation state was streamlined by concurrent operations in the A and B rings. Remarkably, Hagiwara appears to have avoided the epimerization of C8 during the end-game, although the 40% yield in lactone formation may reflect an epimeric byproduct. This

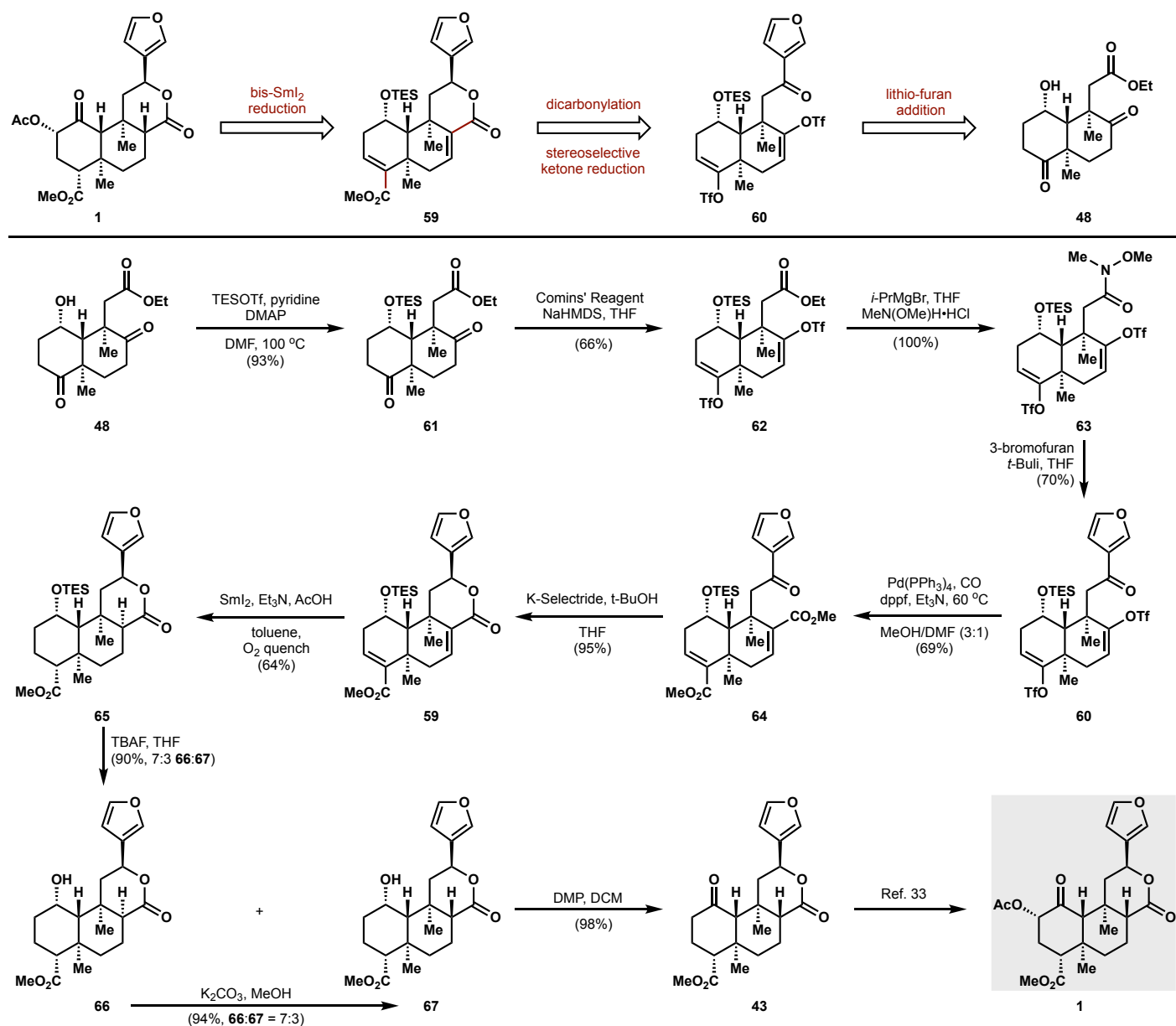


**Figure 6.** Hagiwara's second generation synthesis revised the C-ring synthesis.

epimerizable carbon, however, prevented direct installation of the final acetoxy group and required a three-step workaround. Hagiwara's second-generation synthesis addressed some of these pitfalls.

### 5. Hagiwara's Second Generation Asymmetric Synthesis

Hagiwara published a second synthesis one year later that relied on a similar strategy of parallel C17/C18 oxidation, but sought to overcome the poor dr of the previous 3-lithiofuran addition and to circumvent the many protecting group manipulations that snarled the first route (**Figure 6**).<sup>36</sup>

This second synthesis opened as the first with oxidation of a Wieland-Miescher ketone derivative and reductive alkylation to install an ethyl acetate motif. The hydroxyl group was protected as a

triethylsilylether and doubly triflated with Comins' reagent. The ethyl ester was then converted to its Weinreb amide into which 3-lithiofuran added once. Ketofuran **60** thus circumvents the poor dr of the first route and foists the responsibility of diastereoselective addition onto a hydride reagent—from which there are many to choose. Both enoltriflates were then catalytically carboxylated: recovered mono-carboxylated products were then resubjected to afford the di-methyl ester **64** in high yield. K-Selectride, tasked with delivery of high stereoselectivity, performed admirably, forming tricycle **60** as a single stereoisomer after *in situ* lactonization. Conjugate reduction with SmI<sub>2</sub> afforded tricycle **65**, however with the incorrect stereochemistry at C8—similar to Evans' observations using polar methods. TBAF-mediated deprotection of the TES group led to partial epimerization at C8, and treatment of the undesired epimer with potassium carbonate in

methanol afforded a 7:3 mixture favoring the undesired C8 epimer in 94% yield, which allowed iterative recycling to increase overall yield. Oxidation using Dess-Martin periodinane intercepted previous intermediate **43**, completing a formal synthesis. This synthesis proceeds in 18–20 steps, depending on whether recycling/resubjection steps are included, and improves the overall yield from 0.5–1.4% (with 4x recycling of the C8 epimer).

Hagiwara's second generation synthesis solved the difficult C12 diastereoselectivity problem of the first generation route, however the C8 stereocenter was no longer set early in the synthesis and thus formation of the stereocenter favored the undesired epimer. The synthesis end game still required the arduous C2 oxidation and inversion of stereochemistry.

## 6. Hagiwara's Salvinorin F Synthesis

The Hagiwara group also pioneered syntheses of challenging neoclerodane diterpenoid congeners of SalA, such as salvinorin F **71** (Figure 7).<sup>37</sup> Salvinorin F is a minor metabolite of *S. divinorum* and its biological activity not as extensively studied. Its structure and synthesis could also serve as a key linchpin for the syntheses within the salvinorin family. Salvinorins C-I all contain the same C3 unsaturation as F and additional oxidation in the A ring.

Hagiwara took advantage of his second-generation synthesis of SalA and diversified intermediate **59** to reach salvinorin F. As in the previous synthesis,  $\text{SmI}_2$  effected conjugate reduction of the tricyclic; here, however, a monoreduction is desired. Solvent, proton source and temperature each played a role: toluene and pivalic acid at  $-78^\circ\text{C}$  maintained unsaturation at C3. However, C8 epimers were again produced, and the incorrect stereoisomer predominated 3:1. The minor isomer **69** underwent desilylation with TBAF, buffered with acetic acid to mitigate epimerization, and afforded salvinorin F. The still-protected C8 epimer **68** was subjected to unbuffered TBAF to furnish salvinorin F and its C8 epimer in 82% yield, heavily favoring the incorrect C8 configuration, which could be iteratively recycled with methanolic potassium carbonate (25% **71** per iteration).

Hagiwara's synthesis of salvinorin F was one of the first syntheses of other salvinorin family members and it showcases how divergency of previous SalA syntheses can produce other members of the family where biological activity is underexplored. The synthesis also reiterates the instability of the salvinorin scaffold, with the continued problem of C8 epimerization.

## 7. Forsyth's Asymmetric Synthesis

Another strategy to access SalA relies on the use of an intramolecular Diels-Alder reaction (IMDA) to construct the *trans*-decalin core early in the synthesis. The efficiency and predictability of IMDA reactions allows subsequent risk and effort to be pushed ahead to later steps, either functional group interconversions, C-ring construction or both. The powerful predictability of the Diels-Alder reaction may explain why two groups independently published related, yet distinct, variations on this strategy.

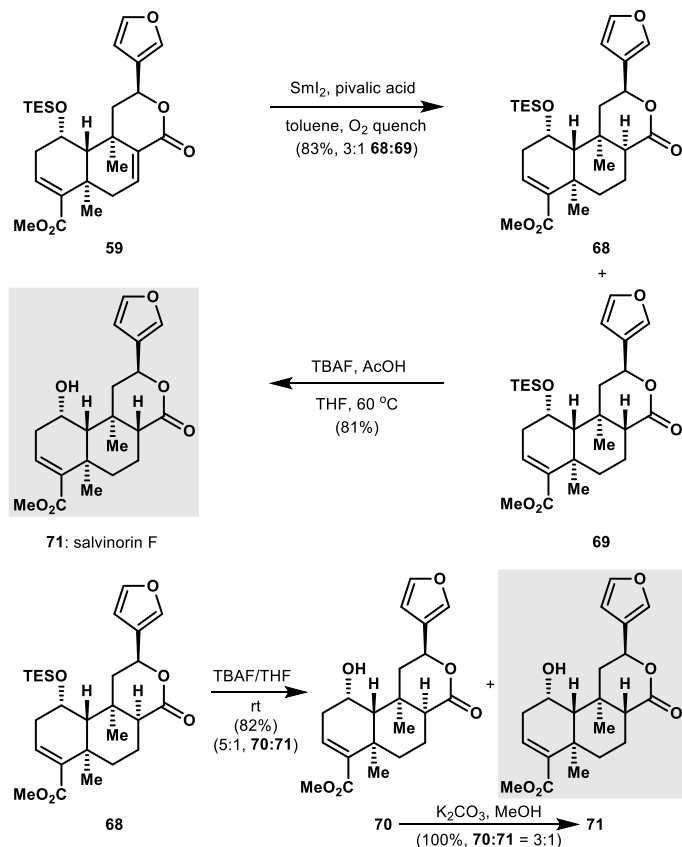


**Figure 7.** Hagiwara's extension to salvinorin F, which suffers the same epimerization problem as salvinorin A.

Forsyth and co-workers were the first to explore the IMDA approach in 2016 (Figure 8).<sup>38</sup> Their route began from tartaric acid derivative **74**—a substructure recognition strategy that allows enantiospecific entry to the synthesis. Efficiency depends, however, on the minimization of functional group interconversions (FGIs) between strategic waypoints: **74**, Diels-Alder cycloadduct **79**, and SalA (**1**). Three other key disconnections are crucial to introduce the remaining stereocenters: (i) double reduction of diene **83**, (ii) diastereoselective addition of (3-furyl) $\text{Ti}(\text{O}i\text{Pr})_3$  with (*R*)-BINOL- $\text{Ti}(\text{O}i\text{Pr})_2$  to aldehyde **72**; and (iii) palladium-mediated decarboxylative allylation. The key Diels-Alder cycloaddition establishes two central stereocenters and is assisted by a dithiane. In contrast to a ketone, the dithiane is believed to minimize allylic strain in the transition state (TS), but also serves as a linchpin to merge diene and dienophile. The stereochemical outcome can be rationalized by a chair-boat TS in which all substituents are pseudoequatorial except for the vinyl methyl group. The reaction was conducted under reflux in 1,2-dichlorobenzene and yielded **80** after oxidation of the dithiane (60% in two steps). Palladium-catalyzed allylation successfully reached the targeted product **81** stereoselectively and in 94% yield, where stereocontrol is justified by steric hindrance. In a major advance for this area, a stereoselective addition of the furan moiety is achieved by addition of a furan-3-titanium alkoxide in the presence of (*R*)-BINOL- $\text{Ti}(\text{O}i\text{Pr})_2$ . Lactonization occurs spontaneously to yield 74% of the

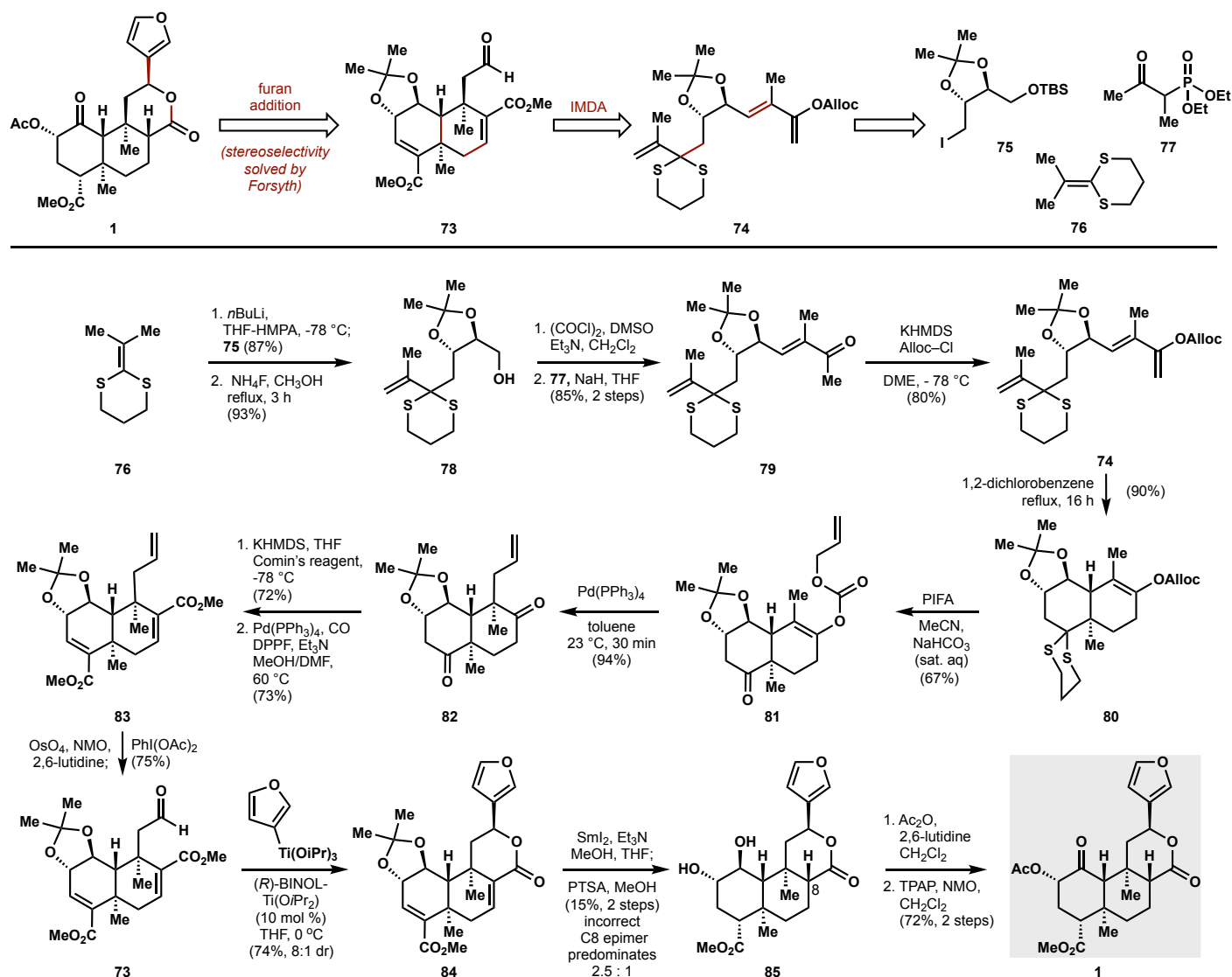


**Figure 8.** Forsyth's synthesis features an intramolecular Diels-Alder reaction to establish the hindered decalin core of SalA

target product in a diastereoisomeric ratio of 8:1, favoring the correct configuration at C12.

The major drawback of this pathway is the endgame, inspired by Hagiwara, whereby double reduction with  $\text{SmI}_2$  yields two diastereomers, epimeric at C8 and favoring the incorrect 8S isomer. Selective acetylation of the 8R product **84** on the hydroxyl group at position C2 and selective oxidation at C1 yields SalA.

## 8. Metz's Synthesis

Metz also explored an IMDA strategy but with an interesting twist in its double application (Figure 9).<sup>39</sup> In contrast to Forsyth, the Metz group began with construction of the lactone ring with correct configurations at C8, C9 and C12 in order to relay stereochemistry to the *trans*-decalin core using an IMDA reaction. The lactone core itself, however, was also constructed with an IMDA.

The Metz group had previously described a route to lactone **86**,<sup>40</sup> which was optimized by use of Liebeskind coupling and prolonged reaction times. The configuration of C8, however, did not correspond SalA. The synthetic route to access **85** transits through **86** and includes a Horner-Wadsworth-Emmons reaction under basic condition sufficient to epimerize C8 partially. However, base leads to isomerization of the (*E*)-enoate and still favors the unproductive *cis*-substituted lactone, which could not be efficiently converted to SalA without generating complex stereoisomeric mixtures. Instead, the 8R diastereoisomer was successfully converted into **85** using a Pd-catalyzed Stille coupling with a vinyl tributylstannane. Triene **85** was dissolved in chlorobenzene along with BHT (2,6-di-*tert*-butyl-4-methylphenol) and warmed to  $200\text{ }^\circ\text{C}$  to produce the desired diastereomer **97**, a precursor of SalA. The *trans* configuration of C8 and C9 leads to an *endo*-chair transition state with the lactone ring in a chair conformation which forms **97**. This cycloaddition



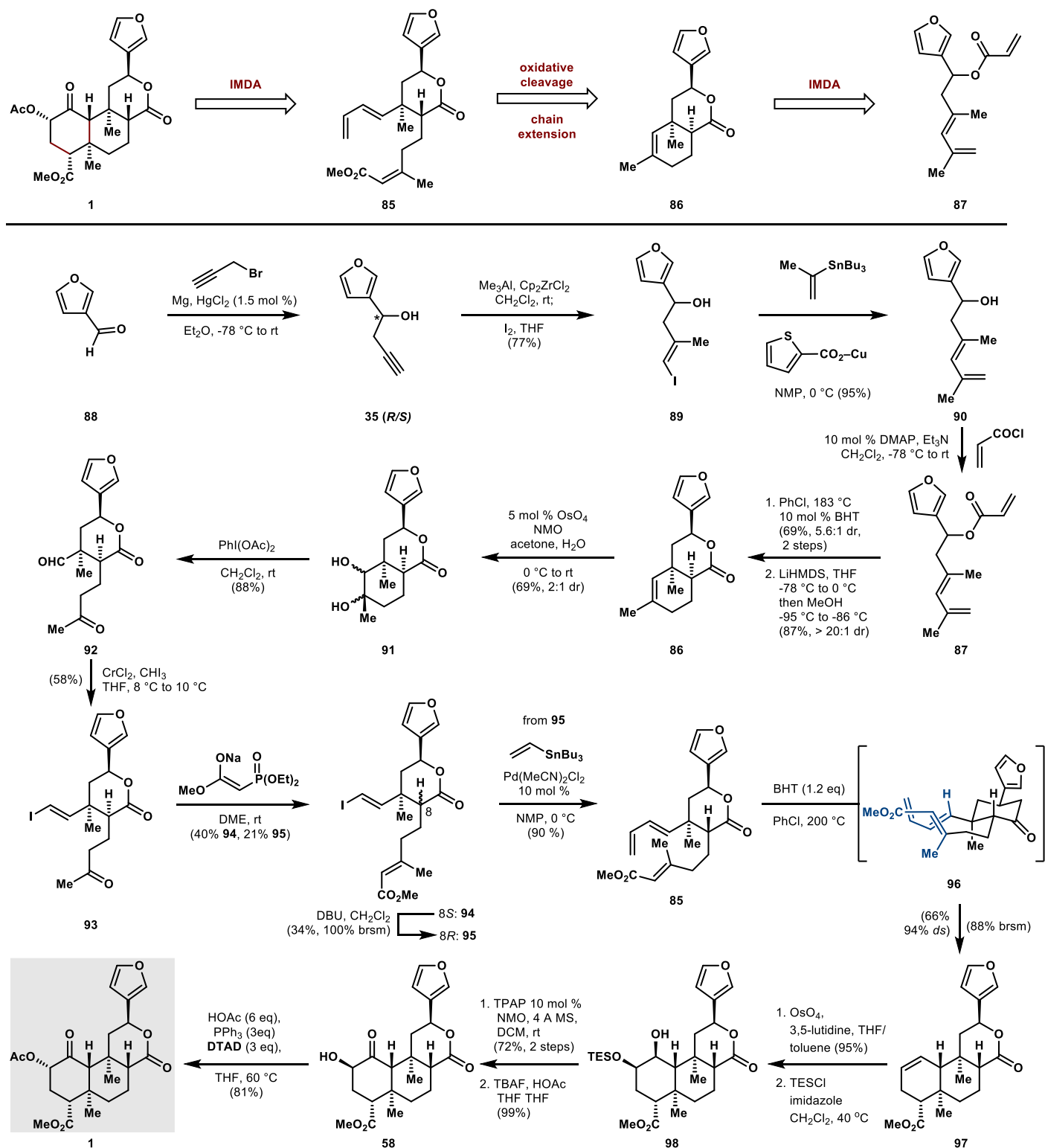


**Figure 9.** Metz's synthesis of SalA featured two intramolecular Diels-Alder reactions to relay stereochemistry from a chiral alcohol

step provides the *trans*-decalin core of SalA with a good selectivity (88%, 94% ds) and sets three stereocenters at C4, C5 and C10. Final

functionalization steps of the cyclohexene include an  $\text{Os}^{\text{VIII}}$ -mediated dihydroxylation, selective silyl-group protection of the alcohol at C2

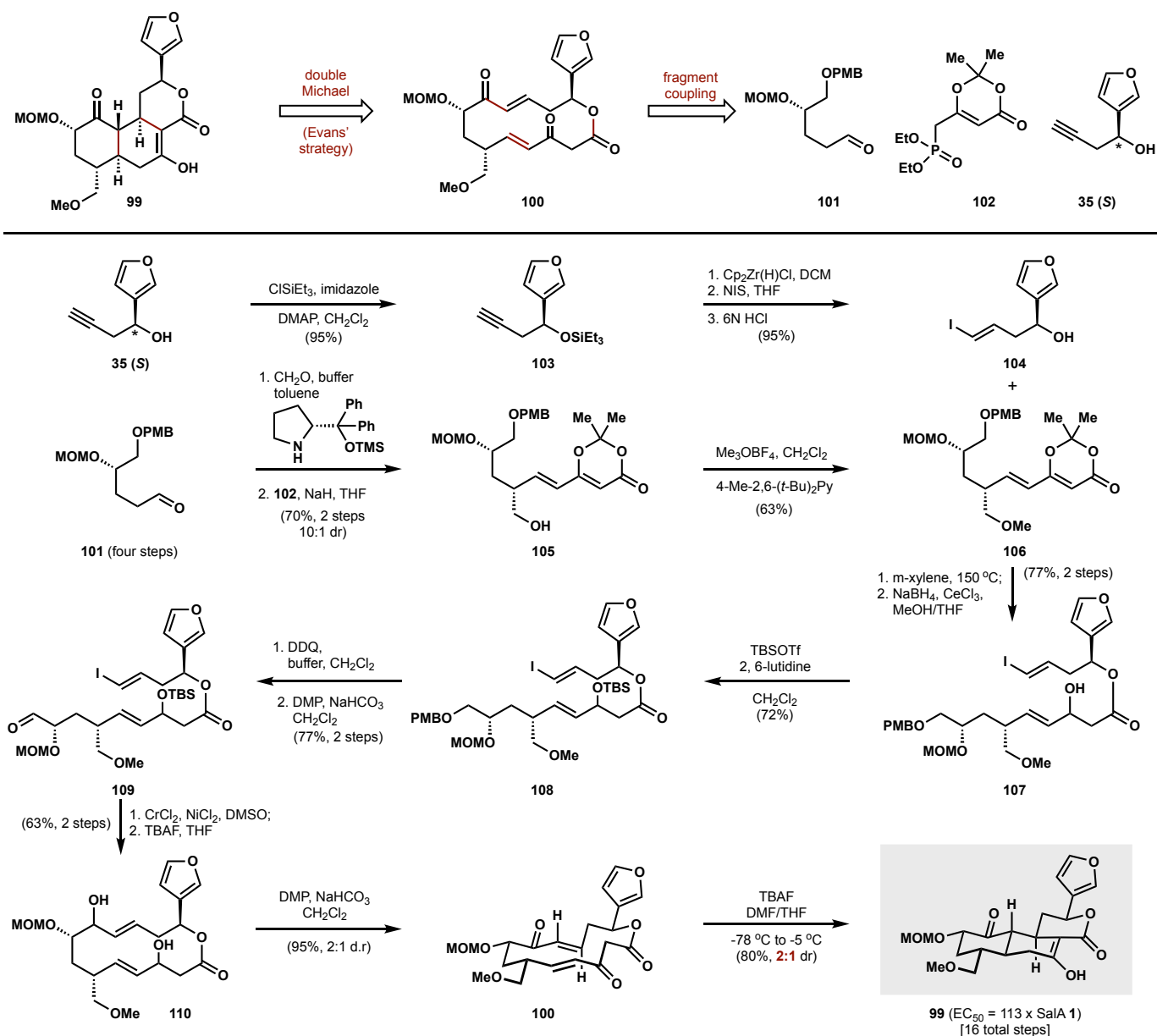


**Figure 10.** Prinsanzano's synthesis parlayed the Evans' transannular Michael cascade into a short route to a moderately active SalA analog.

and a Ley-Griffith oxidation to obtain the ketone at C1. A final Mitsunobu reaction reduces the large excess of reagents used by Hagiwara but has the disadvantage of generating 2-epi-salvinorin A (18 %) along with the desired product (81%).

### 9. Prinsanzano's 16-step Analogue Total Synthesis

As is common in natural product total synthesis, a target selection is justified by biological activity. SalA benefits from extensive literature detailing its study or justifying its importance: over 530 papers are catalogued by Web of Science to contain "salvinorin" as a topic word. Its importance derives from high selectivity and potency at the  $\kappa$ -opioid receptor,<sup>16</sup> its rapid and efficient brain penetration,<sup>41</sup> and in vivo data from animals as well as humans due to recreational use.<sup>42,43</sup> Many papers describe structure-activity

relationships, and the Prinsanzano group has been a leader in this area, producing diverse analogues through semi-synthesis, many with surprising and useful properties.<sup>44,45,46,47</sup> Some generally accepted findings are: substitution at the C4 ester often lowers activity and the carboxylic acid is completely inactive;<sup>48</sup> heteroatom substitution at C2 is necessary for activity, but can be improved by a metabolically stable methoxy methyl (MOM) ether, as opposed to a labile acetate;<sup>21</sup> the furan is crucial, as its removal ablates activity (hydrogen bonding was proposed as a preferred interaction,<sup>49</sup> but subsequently disproven,<sup>17</sup> see Section 10); structural changes to the C-ring (lactol or cyclic ether) retain potency within one order of magnitude, but diverse C-ring modifications have been difficult to obtain through semi-synthesis.<sup>50</sup>

Given these findings, the Prinsanzano group proposed a 3-point binding model of SalA involving the C2 acetate, C4 ester, and

C12 furan. They sought to leverage this knowledge to produce a concise and diversifiable synthesis of the SalA scaffold and explore its pharmacology with greater flexibility than what is possible through semi-synthesis. The C19 and C20 methyls were assumed to be unimportant for binding—a question not yet addressed by the earlier Perlmutter work—and the synthetically-required B-ring ketone was retained. This main target, **99**, dubbed a “pseudo neoclerodane,” relied on Evans’ synthetic strategy for its construction (**Figure 10**). Retention of oxidation at C7 reduced the number of steps, but introduced some uncertainty since its effect on binding was unexplored.

Aldehyde **101**, available in 4 steps,<sup>51</sup> was subjected to hydroxymethylation under Boeckman conditions<sup>52</sup> and a subsequent Horner-Wadsworth-Emmons reaction with phosphonate **102** (also described by Boeckman) arrived at intermediate **105** in good yield and dr.<sup>53</sup> Methylation and thermolysis of **105** in xylenes at 150 °C generated a ketene which was captured furyl alcohol **104** to furnish ester **107**, after NaBH<sub>4</sub> reduction. Three functional group interconversion led to the precursor of Nozaki-Hiyama-Kishi macrocyclization, which was effected by 10 equiv. CrCl<sub>3</sub> and 0.02 equiv. NiCl<sub>2</sub>, to yield an inconsequential mixture of diastereomers in 63% yield. Oxidation with Dess-Martin periodinane converted the allylic alcohol into a Michael acceptor that was poised to undergo Evans’ transannular cascade cyclization upon treatment of **100** with TBAF. The reaction occurred in good yield, but **99** was contaminated with a stereoisomer (33%) that either derived from impure **100** or poor stereocontrol in the Evans cascade. It should be noted that step counting in this report combines multistep reactions separated by solvent distillation, aqueous workup and filtration; more orthodox enumeration of steps expands the nine steps noted in the abstract to sixteen.

The last question to be answered by Prisinzano was whether these analogues had potential to be active. Target **99** was assayed for *kappa*-opioid receptor potency and compared to SalA itself, as well as the endogenous opioid peptide dynorphin A. Unfortunately, **99** displayed over 100-fold loss in activity. Such a variation was not clearly assignable since so many structural changes separate **99** from SalA. So, a promising start to new SalA analogues has been uncovered, but refinements to the synthesis and significant gains in potency are necessary before a powerful platform for pharmacology can be realized.

#### 10. Shenvi’s 20-nor-SalA and O6C-20nor-SalA Synthesis

Our group sought to address the salvinorin problem informed by the persistent issue of C8 epimerization—which scuttled total synthesis and semi-synthesis campaigns, as noted above. At the time, however, the driving force for C8 epimerization had not been identified. We hypothesized two driving forces: 1,3-diaxial strain between the C20 methyl and the C12 hydrogen, which is relieved by C8 epimerization; and increased planarization of the C-ring lactone, whose CO—C=O dihedral angle is decreased in the *cis*-ring junction. Therefore two scaffold changes—C20 replacement with H and lactone replacement with cyclohexane—were applied to SalA. In essence, these changes took the place of initial retrosynthetic transforms to

reduce synthetic complexity, but corresponded to ‘nonsense’ steps to stabilize the scaffold. In fact, C20 methyl deletion achieved both: the scaffold was predicted to favor the correct C8 configuration and, even though structural complexity remained the same, a short route appeared to open.

A Michael disconnection that would have been difficult and stereochemically confounding emerged through C20 deletion and simplified synthetic access. However, the benefits of scaffold stabilization and rapid synthetic access depended entirely on whether this modification significantly affect engagement of the KOR. This risk was partly mitigated by docking studies that suggested C20 pointed away from the binding pocket and therefore its deletion would be unlikely to affect binding. Retrosynthetic dissection involved lactonization, Heck arylation and intramolecular Michael reaction. Establishment of stereochemistry in the Michael reaction relied heavily on the stabilization imparted by methyl deletion: in this step and installation of the C2 acetoxy group, base-mediated equilibration of stereochemistry was achieved. The Michael precursor resembled a vicinally difunctionalized Hagemann’s ester, consequently targeted as the starting material (**Figure 11**).

Commercially available Hagemann’s ester was first advanced by conjugate addition of Grignard reagent **115**—transmetalated to copper—followed by trapping with acrolein, incorporating almost all skeletal carbons in a single step. Elimination of the secondary allylic alcohol gave enone **117** primed as a Michael acceptor. Deprotection of the primary TBS group and oxidation to the aldehyde allowed application of standard pyrrolidine catalysis conditions. Although both diastereomers of the intermediate bicycle were produced, scaffold stabilization allowed *in-situ* epimerization with potassium carbonate and funneled the reaction towards the thermodynamic *trans*-decalin in high yield. The same thermodynamic stability was leveraged to set the C2 acetoxy stereochemistry, which was accomplished by LDA enolization and Davis oxaziridine hydroxylation, followed by *in situ* acetylation; epimerization occurred in the same step when DBU was used as base. One key nuance here is that Pinnick oxidation preceded this C2 oxidation to prevent competitive hydroxylation of the aldehyde, but use of a free carboxylic acid across these steps proved operationally challenging. The redeeming feature of this nuisance came in the form of furan installation. Many attempts to arylate the alkene in the presence of the aldehyde or at different stages of the sequence remained unsuccessful. The carboxylate, however, proved uniquely effective to promote Heck arylation with 3-bromofuran—an unprecedented directing group effect in Heck arylation and one that has since been expanded to robust methodology to form quaternary carbons.<sup>54</sup> A potassium cation proved the most effective to realize high yields, consistent with the Yu model for η-2 potassium chelation and coordination of palladium *cis* to the alkenyl sidechain.<sup>55</sup> Stereoselective lactonization provided 20-nor-salvinorin A, but only after extensive screening. C-O bond formation was found to be reversible, leading to equilibration of diastereomers using Bronsted and Lewis acids. In contrast, HFIP was thought to acidify the carboxylic acid of **120** and promote internal protonation followed by ion collapse, generating a 4:1 diastereomeric mixture in favor of the correct C12 configuration. This 10-step synthesis produced

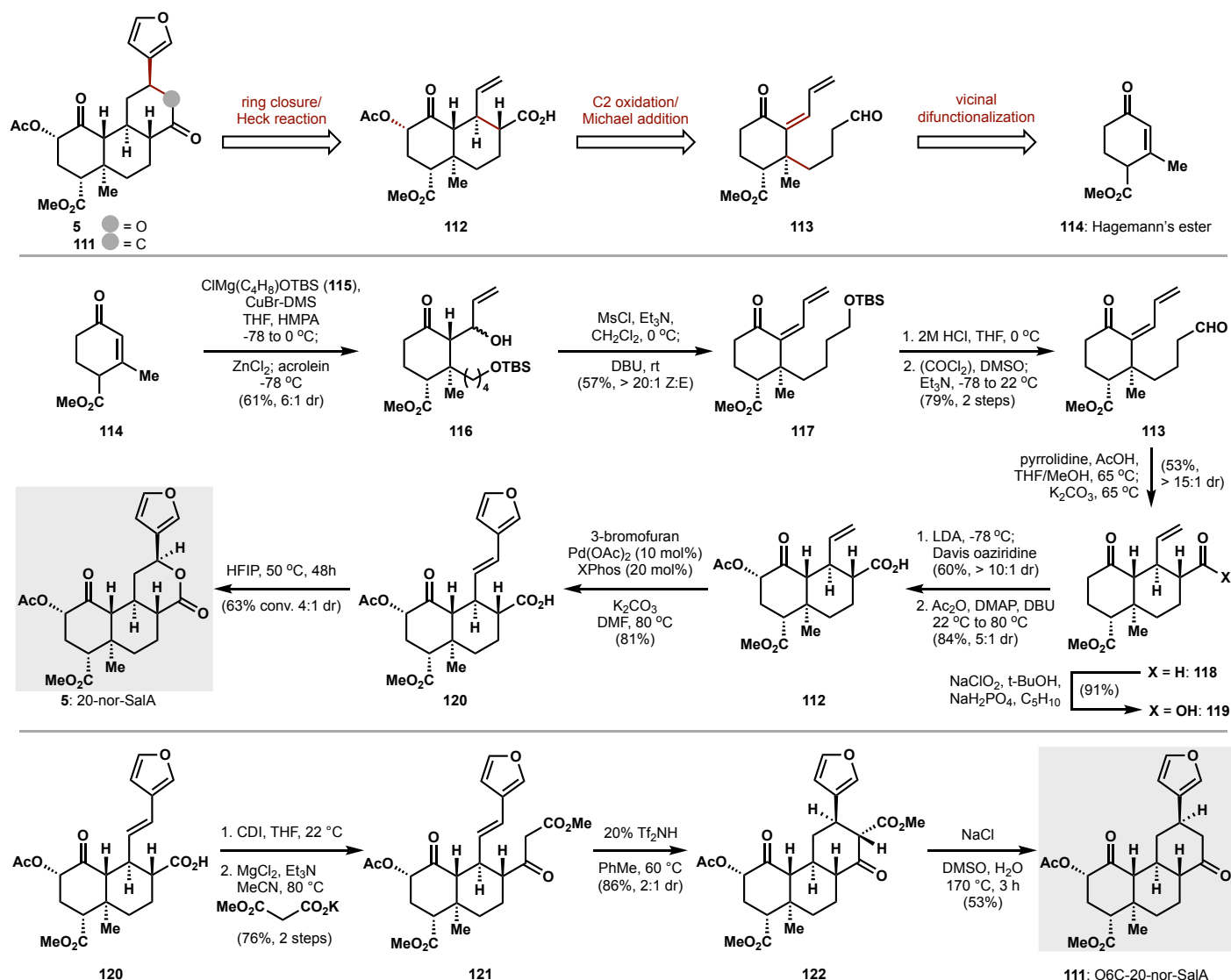


**Figure 11.** Shenvi's synthesis of SALA analogs that retain high potency and selectivity at KOR but remove epimerization.

20-nor-salvinorin A in a 3% overall yield, but its value hinged on any improved scaffold stabilization and its affinity at the KOR.

Epimerization studies with DBU in d3-MeCN revealed that 20-nor-sal-A reversed the stability of SalA and its C8 epimer. So, whereas SalA decreased to 30% with 8-epi-SalA growing to 70%, nor-20-SalA generated only 30% of its C8 epimer. Assays of 20-nor-sal A revealed affinity and potency about 5-fold lower than SalA itself, and with the same high selectivity for KOR over MOR and DOR. Notably, these assays compared *rac*-nor-20-SalA to *nat*-SalA, suggesting that a single enantiomer of nor-20-SalA might exhibit higher potency. Several other C12 aryl analogues were generated, showcasing how the synthesis is easily diversifiable. Interestingly, the phenyl analogue exhibited comparable activity to 20-nor-Sal A, calling into question a proposal that a hydrogen bond to the furanyl oxygen significantly contributed to potency.<sup>56</sup>

In addition to 1,3-diaxial strain imparted by the C20 methyl, our group identified a dihedral angle driving force for C8 epimerization and designed a synthesis of O6C-20-nor-sal A, replacing the C ring lactone with a cyclic ketone.<sup>57</sup> The synthesis diverged from

the prior intermediate **120**. DCC coupling afforded beta-keto-ester **121** which would allow the enol tautomer to predominate and simplify acid-mediated cyclization onto the benzylic alkene—a more difficult task than carboxylic acid cyclization due to keto-enol tautomerism. Cyclization was realized by treatment with triflimide and provided a 2:1 diastereomeric mixture, in favor of the equatorial furan stereochemistry. Final Krapcho decarboxylation of the ester yielded O6C-20-nor-sal A.

As predicted, O6C-20-nor-sal A does not epimerize at all in basic conditions. In addition, it lost no potency towards KOR agonism compared 20-nor-SalA itself and exhibited the same balanced agonism as the benchmark agonist U69,593, i.e. no bias for G protein signaling versus  $\beta$ -arrestin recruitment. This increased stability, high potency and room to improve bias established O6C-20-nor-SalA as a promising scaffold for a medicinal chemistry campaign. The ketone functionality also serves as a new handle for modifications that would not be possible from the lactone moiety. Such a campaign would require a robust and diversifiable synthesis of the scaffold. The route to O6C-20-nor-sal A here is concise but many late stage steps are low yielding,

and the overall synthesis racemic, which challenges a serious SAR exploration. Rendering these syntheses asymmetric is challenged by the tendency of Hagemann's ester to epimerize and is the subject of ongoing efforts.

### 11. Comparison of routes through chemical space

The benefits of one chemical synthesis over another can be judged by metrics used in the pharmaceutical industry like process mass intensity (PMI, industrial scale), cost, labor, impurity profile and environmental impact; as well as less rigorous metrics preferred in academia like step count or yield per step, neither of which are carefully regulated. This sort of verdict is problematic for a naturally abundant molecule whose mere production is not the priority. If, instead, the structure must be optimized toward functional endpoints, then different routes can serve different purposes: one route quickly produces a diversifiable scaffold, another route convergently merges building blocks; both may access orthogonal libraries. For this review, comparison is complicated by the targeting of 4 different scaffolds for future development—SalA, Prisanzano's *pseudo*-neoclerodane, nor20SalA and O6Cnor20SalA. Since these scaffolds and any of their intermediates might be diversified to structurally-similar opioid receptor agonists, we analyzed how the routes navigate chemical space approaching the target. The idea is that rapid access to similar compounds (close in NP chemical space, if properly defined) can serve as a platform for future biological discovery.

Chemical space defined by **x**: Tanimoto coefficient (similarity to target),  
**y**: oxidation state, **z**: complexity index (Cm)

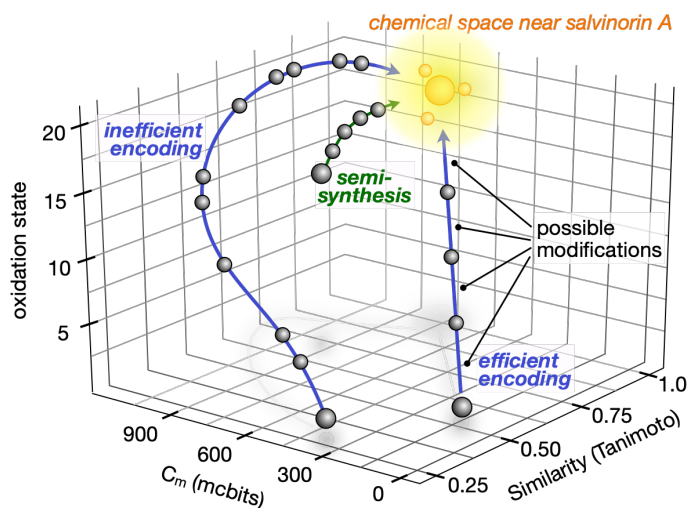


**Figure 12.** Choice of dimensions for visualizing movement through a chemical space during total synthesis.

We chose three dimensions to define chemical space through the course of these syntheses (Figure 12). The first dimension was depicted by Tanimoto index using the SkeletonSphere's descriptor in the DataWarrior software package. This dimension can quantitatively differentiate 'total synthesis' from 'semi-synthesis' by measuring similarities between graphs of chemical bonding. For the purposes of the analysis here, where there are no semi-syntheses, the Tanimoto index dimension can gauge how soon and how rapidly the commercial materials begin to approach salvinorin chemical space, which greatly

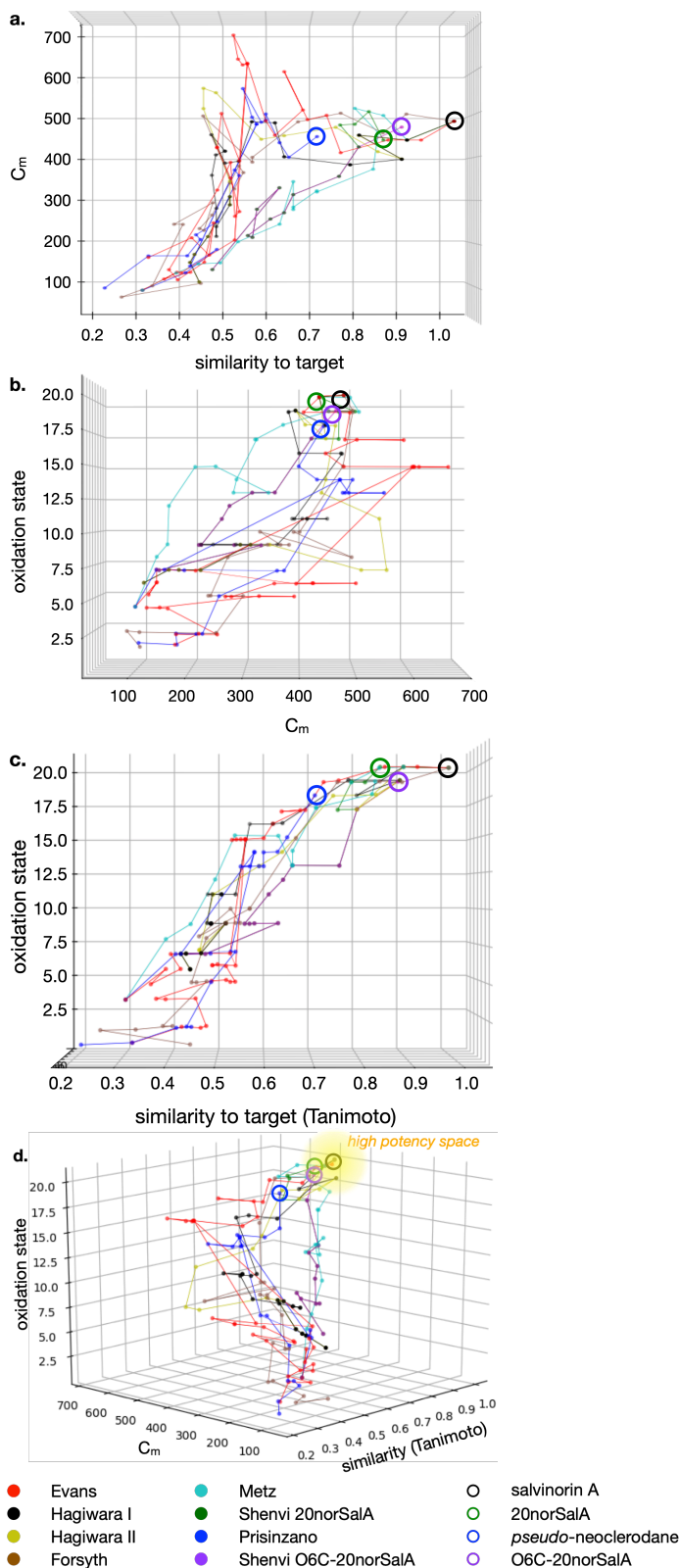


**Figure 13.** Syntheses traversing a chemical space: **a.** information content (Cm) vs. target similarity (Tanimoto), **b.** oxidation state [O] vs. Cm, **c.** [O] vs. Tanimoto, **d.** [O] vs. Cm vs. Tanimoto.

impacts the efficiency of encoding the information content necessary for bioactivity. The second dimension measures information content according to the Böttcher index  $C_m$ , which is an additive measure of how all atoms are connected.<sup>58</sup> Unlike the Tanimoto index,  $C_m$  can exceed the target if a synthesis overshoots complexity by addition of too many atoms, extra stereocenters or auxiliary rings. Instead, incremental increase in  $C_m$  with few nodes (intermediates) between starting material and target can signal efficient encoding of complexity. Annotation of  $C_m$  for each intermediate was significantly accelerated by a Python script written by Professor Stefano Forli.<sup>59</sup> The third dimension measured skeletal carbon oxidation state (specifically the number of the skeletal carbons at the correct oxidation state in a particular intermediate) to visualize how redox reactions are used productively. Since oxygenation patterns impact binding affinity, stability and metabolism,<sup>20</sup> their efficient encoding within the synthesis effects how these functional attributes of the target can be perturbed.

First, we assembled three graphs to look for similar patterns between syntheses, as well as any redundancies between the dimensions. There was an overall weak positive correlation between complexity ( $C_m$  score) and similarity to target (Tanimoto index): these are non-redundant measures (Figure 13a). Many syntheses rapidly reach high information content, or overshoot complexity, without nearing structural similarity. The simplest syntheses show a linear correlation between complexity and similarity – little is wasted in approach of the target. Similarly, oxidation state and  $C_m$  (Figure 13b) showed little overall correlation, but the most straightforward syntheses showed a generally linear correlation between oxidation state and complexity. In contrast, oxidation state directly correlated to target similarity. Many of the less efficient syntheses, however, reached a scaffold one or two oxidation states away and still required several steps to reach the target, either installation of the final oxidations or carrying out several redox redundant FGIs.

Put together into Figure 13d, the syntheses partition into two groups: Metz/ 20norSalA versus all others. This graphical separation reflects three main attributes: 1) absence of auxiliaries, protecting groups, unproductive stereocenters or functional groups—all of which add information content ( $C_m$ ) without approaching target similarity; 2) early access to oxidized intermediates that elevate the syntheses above the scrum of functional group interconversions that bog down other routes; and 3) relatively few steps that separate these simple, highly-oxidized intermediates from their targets. These relationships suggest that future work should focus on direct access to a highly oxygenated framework, where oxidation state is embedded in starting materials.

## 12. Scaffold Hopping vs. Dynamic retrosynthesis

Natural products (NPs) are excellent starting points for drug discovery as they typify topologically complex small molecules, which tend to exhibit greater specificity of protein binding.<sup>60</sup> Natural products are not, however, rendered flawless by evolution, especially since natural selection pressures do not include clinical trials! Instead, the target could be thought of as dynamic, subject to structural change that maintains its unique, natural product character (locus in chemical space), but opens concise synthetic paths and improves functional liabilities. Scaffold changes not only alter retrosynthesis, but can improve diversifiability for SAR studies, enhance metabolic stability, adjust distribution and refine other pharmacokinetic profiles. This idea of treating the normally static target of a retrosynthetic analysis as dynamic is related to the idea of scaffold hopping in medicinal chemistry. The term “scaffold hopping” was originally coined in 1999 by Schneider,<sup>61</sup> but remains poorly defined in the literature. The concept broadly refers to taking inspiration from a lead compound or

its main pharmacophore and changing the scaffold to arrive at novel chemotype with improved bioactivity, altered pharmacokinetic profiles and open intellectual property rights. Scaffold-hopping among opioids is commonplace and typified by tramadol, a pain reliever, which was designed from the powerful opioid morphine.<sup>62</sup> The tramadol scaffold, however, has lost three out of five rings and three out of five stereocenters. It has a lower potency than morphine but also reduced side-effects, importantly attenuating respiratory depression compared to morphine.<sup>63</sup> In contrast, SalA, 20-nor-SalA and O6C-20-nor-SalA all possess nearly identical scores—probably not far enough to be considered a hop. While dynamic analysis is still being developed, scaffold-hopping has been classified into four main categories: heterocycle replacements, ring opening or closure, peptidomimetics and topology-based hopping.<sup>51</sup> Like dynamic analysis, these approaches are usually computationally aided: several programs have been developed to aid scaffold-hopping, including CATS, used by Schneider.<sup>50</sup> The distinguishing feature between scaffold-hopping and dynamic retrosynthesis, aside from an emphasis on complex NPs, is maintenance of chemotype rather than movement (hopping) to a different scaffold. Quantitatively comparing changes in complexity scores, developed by Böttcher,<sup>56</sup> between tramadol and morphine, and Sal and O6C-20-nor-SalA, it is clear that tramadol loses a significant amount of complexity 38% from the scaffold hop, whereas O6C-20-nor-SalA only loses 4% complexity in the dynamic analysis. However, both methods produce compounds with maintained bioactivity and simplified synthetic approaches (Figure 14). Scaffold hopping may prove to be an important and complementary approach to dynamic analysis in total synthesis if two NP chemotypes share a target, but one is underexplored or more accessible. Given the importance of the kappa-opioid receptor, its homology to other GPCRs and the complexity of the SalA chemotype, scaffold hopping to other NPs known to engage homologous GPCR binding sites may provide a fruitful range of targets to explore. Indeed, several metabolites have shown promising activity at kappa- and mu-opioid receptors.<sup>64,65</sup>

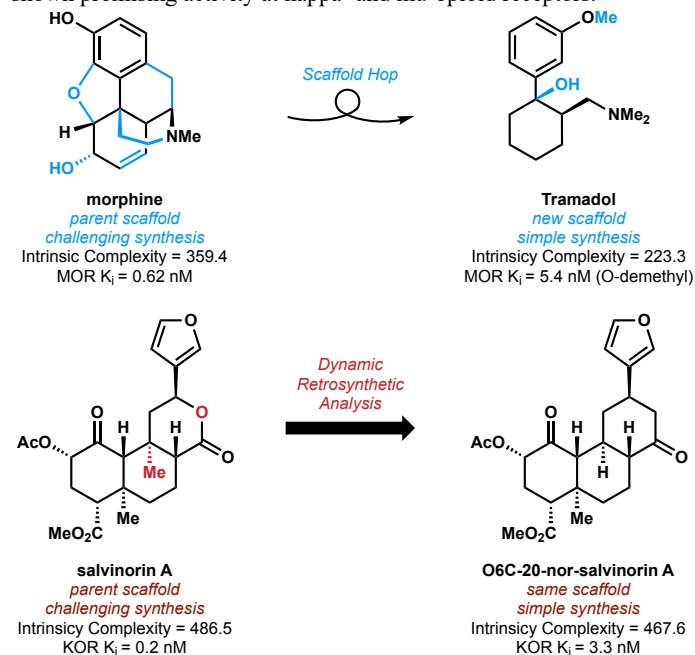


**Figure 14.** Scaffold hopping versus scaffold preservation/ alteration to reduce synthetic burden in natural product space.



### 13. Conclusions

SalA has emerged as a promising candidate for development of KOR-selective tool compounds and novel therapeutics: as an anti-preuritic, analgesic or rapid-acting/ rapid-resolving hallucinogen. Further advances in this area could be significantly enabled by efficient and diversifiable syntheses. As discussed in the preceding sections, all the previous syntheses of SalA were plagued by epimerization of the C8 carbon, which we identified as driven by 1,3-diaxial steric clash, combined with lactone planarity, and supported with experimental data derived from total synthesis. In addition to scaffold instability, SalA possesses metabolic liabilities: the C2 acetate is subject to cleavage by carboxyl esterases and the C-ring lactone is subject to ring-opening by calcium lactonases, the metabolites being less-potent or inactive compounds like salvinorin B.<sup>66</sup> The furan is proposed to be labile to oxidation.<sup>47</sup> SalA also does not distribute well for an ideal chronic pain medication, as it acts in both the peripheral and central nervous system, quickly penetrates the blood brain barrier and can cause intense hallucinations and dysphoria. A growing body of opioid research has proposed that peripherally restricted opioids can prevent the psychological side-effects that often accompany the local analgesia. Robust support for this idea comes from the recent successes of difelikefalin, a peripherally restricted KOR agonist, in phase III and II clinical for uremic pruritis<sup>67</sup> (internal itch due to kidney failure) and acute postoperative pain,<sup>68</sup> respectively.

Stabilization of the salvinorin A scaffold by substituent replacement and scaffold editing has established a powerful foundation for future work. Chemical innovations projected for the future include further efficiency gains in development of a high-yielding, asymmetric route; application of combinatorial methods to generate large, diverse libraries; and appendage of groups for binding-site elucidation<sup>54</sup> or photopharmacology.<sup>69</sup> Biological innovations include increased oral bioavailability, peripheral restriction, increased brain-residence time and biased signaling. The diversity and importance of challenges arrayed against the salvinorin A chemotype promise many discoveries wait just beyond the horizon.

**14. Acknowledgements.** S.J.H. is a Skaggs Fellow, Dean's Fellow and Postgraduate Scholar-Doctoral (PGS-D) supported by the National Sciences and Engineering Research Council of Canada (NSERC). R.A.S. acknowledges the generous support of the National Institutes of Health (R35 GM122606) and the National Science Foundation (CHE-1856747), as well as a generous Scientific Advancement Grant from Boehringer-Ingelheim.

**Sarah Hill** is a doctoral student in chemistry at Scripps Research. She completed her HBSc at the University of Toronto in 2018 and then joined the Shenvi Lab. Her research is focused on the syntheses of novel salvinorin A scaffolds for applications in medicinal chemistry.



**Aurélien Brion** is a M.Sc. student in chemistry and life sciences at Paris Sciences et Lettres University, Paris, France. After completing his B.Sc. in physical and molecular chemistry at Université Paris-Sud, Orsay, France (2018), he joined the Shenvi Lab at The Scripps Research Institute to complete his Master's thesis about a novel total synthesis of salvinorin A. His main research interests revolve around total synthesis of natural products, biocatalysis and directed evolution of enzymes.



**Ryan Shenvi** is Professor of Chemistry at the Scripps Research Institute in La Jolla, California. His laboratory develops new methods to access bioactive secondary metabolites from chemical feedstocks. Recently his group has started to treat natural products as loci in broader bioactive chemical space: small structural perturbations are made to retain general location and activity but open efficient synthetic paths. Current areas of research include MHAT catalysis, cross-coupling, neuroactive small molecules and reactive pharmacophores.



## References

- Morone NE, Weiner DK. "Pain as the fifth vital sign: exposing the vital need for pain education" *Clin Ther.* 2013;35(11):1728-1732. doi:10.1016/j.clinthera.2013.10.001
- Center for Behavioral Health Statistics and Quality (CBHSQ). *2017 National Survey on Drug Use and Health: Detailed Tables*. Rockville, MD: Substance Abuse and Mental Health Services Administration; 2018
- CDC/NCHS, *National Vital Statistics System*, Mortality. CDC WONDER, Atlanta, GA: US Department of Health and Human Services, CDC; 2018. <https://wonder.cdc.gov>
- Al-Hasani R.; Bruchas M. R. "Molecular Mechanisms of Opioid Receptor-Dependent Signaling and Behavior" *Anesthesiology.* **2011**, *115*, 1363–1381.
- Pathan, H.; Williams, J.; "Basic opioid pharmacology: an update" *Br. J. Pain.* 2012, *6*, 11–16.
- Zjawiony, J. K.; Machado, A. S.; Menegatti, R.; Gedingi, P. C.; Costa, E. A.; Pedrino, G. R.; Lukas, S. E.; Franco, O. L.; Silva, O. N.; Fajemiroye, J. O. "Cutting-Edge Search for Safer Opioid Pain Relief: Retrospective Review of Salvinorin A and Its Analogs" *Front. Psychiatry*, **2019**, *10*, 1–11.
- Valentino, R. J.; Volkow, N. D. "Untangling the complexity of opioid receptor function" *Neuropsychopharmacology*, **2018**, *43*, 2514–2520 b. Pradhan, A. A.; Smith, M. L.; Kieffer, B. L.; Evans, C. J. "Ligand-directed signaling within the opioid receptor family" *Br. J. Pharmacol.* **2012**, *167*, 960–969.
- Che, T.; Majumdar, S.; Zaidi, S. A.; Ondachi, P.; McCorvy, J. D.; Wang, S.; Mosier, P. D.; Uprety, R.; Vardy, E.; Krumm, B. E.; Han, G. W.; Lee, M. Y.; Pardon, E.; Steyaert, J.; Huang, X. P.; Strachan, R. T.; Tribo, A. R.; Pasternak, G. W.; Stevens, R. C.; Cherezov, V.; Katritch, V.; Wacker, D.; Roth, B. L. "Structure of the Nanobody-Stabilized Active State of the Kappa Opioid Receptor" *Cell*, **2018**, *172*, 56–67.
- Reiter E.; Ahn S.; Shukla A. K.; Lefkowitz, R. J. "Molecular Mechanism of  $\beta$ -Arrestin-Biased Agonism at Seven-Transmembrane Receptors" *Annu. Rev. Pharmacol. Toxicol.* **2012**, *52*, 179–197.
- Pfeiffer, A.; Brantl, V.; Herz, A.; Emrich, H. M. "Psychotomimemesis Mediated by  $\kappa$  Opiate Receptors" *Science*, **1986**, *233*, 774–776.
- Brust, T. F.; Morgenweck, J.; Kim, S. A.; Rose, J. H.; Locke, J. L.; Schmid, C. L.; Zhou, L.; Stahl, E. L.; Cameron, M. D.; Scarry, S. M.; Aube, J.; Jones, S. R.; Martin, T. J.; Bohn, L. M. "Biased agonists of the kappa opioid receptor suppress pain and itch without causing sedation and dysphoria" *Science Signaling*, **2016**, *9*, 117.
- Land, B. B.; Bruchas, M. R.; Schattauer, s.; Giardino W.J.; Aita, M.; Messinger, D.; Hnasko, T. S.; Palmiter, R. D.; Chavkin, C. "Activation of the kappa opioid receptor in the dorsal raphe nucleus mediates the aversive effects of stress and reinstates drug seeking" *Natl. Acad. Sci. U.S.A.* **2009**, *106*, 19168–19173.
- Bohn, L. M.; Gainetdinov, R. R.; Caron, M. G. "G Protein-Coupled Receptor Kinase/ $\beta$ -Arrestin Systems and Drugs of Abuse" *NeuroMolecular Medicine*, **2004**, *5*, 41–50.
- White, K. L.; Robinson, J. E.; Zhu, H.; Diberto J. F.; Polepally, P. R.; Zjawiony, J. K.; Nichols, D. E.; Malanga, C. J.; Roth, B. L. "The G protein-biased  $\kappa$ -opioid receptor agonist RB-64 is analgesic with a unique spectrum of activities in vivo" *J. Pharmacol. Exp. Ther.* **2015**, *352*, 98–109.
- Prisinzano, T.; Rothman, R. B. "Salvinorin A Analogs as Probes in Opioid Pharmacology" *Chem. Rev.* **2008**, *108*, 1732–1743.
- Roth, B. Baner, K.; Westkaemper, R.; Siebert, D.; Rice, K. C.; Steinberg, S.; Ernsberger, P.; Rothman, R. B. "Salvinorin A: A potent naturally occurring nonnitrogenous  $\kappa$ -opioid selective agonist" *PNAS*, **2002**, *99*, 11934–11939.
- Roach, J. J.; Sasano, Y.; Schmid, C. L.; Zaidi, S.; Katritch, V.; Stevens, R. C.; Bohn, L. M.; Shenvi, R. A. "Dynamic Strategic Bond Analysis Yields a Ten-Step Synthesis of 20-nor-Salvinorin A, a Potent  $\kappa$ -OR Agonist" *ACS Cent. Sci.* **2017**, *3*, 1329–1336.
- Surratt, C.; Johnson, P.; Moriwaki, A.; Seidleck, B.; Blaschak, C.; Wang, J.; Uhl, G. "-mu opiate receptor. Charged transmembrane domain amino acids are critical for agonist recognition and intrinsic activity" *J. Biol. Chem.* **1994**, *269*, 20548–20553.
- Kane, B. E.; Svensson, B.; Ferguson, D. M. "Molecular recognition of opioid receptor ligands" *AAPS J.* **2006**, *8*, 126–137
- Roach, J. J.; Shenvi, R. A. "A review of salvinorin analogs and their kappa-opioid receptor activity." *Bioorg. Med. Chem. Lett.* **2018**, *28*, 1436–1445.
- Wang, Y.; Chen, Y.; Xu, W.; Lee, D. Y. W.; Ma, Z.; Rawls, S. M.; Cowan, A.; Liu-Chen, L. "2-Methoxymethyl-Salvinorin B Is a Potent  $\kappa$  Opioid Receptor Agonist with Longer Lasting Action in Vivo Than Salvinorin A" *J. Pharmacol. Exp. Ther.* **2008**, *324*, 1073–1083.
- Yan, F.; Bikbulatov, R.V.; Mocanu, V.; Dicheva, N.; Parker, C.E.; Wetsel, W.C.; Mosier, P.D. Westkaemper, R.B. Allen, J.A.; Zjawiony, J.K.; Roth, B.L. "Structure-based design, synthesis, and biochemical and pharmacological characterization of novel salvinorin A analogues as active state probes of the kappa-opioid receptor" *Biochemistry*, **2009**, *48*, 6898–908.
- Beguín, C.; Richards, M. R.; Li, J.; Wang, Y.; Xu, W.; Liu-Chan, L.; Carlezon, W. A.; Cohen, B. M. "Synthesis and in vitro evaluation of salvinorin A analogues: Effect of configuration at C(2) and substitution at C(18)" *Bioorg. Med. Chem. Lett.* **2006**, *16*, 4679–4685.
- Munro, T. A.; Rizzacasa, M. A.; Roth, B. L.; Toth, B. A.; Yan, F. "Studies toward the Pharmacophore of Salvinorin A, a Potent  $\kappa$  Opioid Receptor Agonist" *J. Med. Chem.* **2005**, *48*, 345–348.
- Lingham, A. R.; Huegel, H. M.; Rook, T. J. "Studies Towards the Synthesis of Salvinorin A" *Aust. J. Chem.* **2006**, *59*, 340–348.
- Bergman, Y. E.; Mulder, R.; Perlmutter, P. "Total Synthesis of 20-Norsalvinorin A. 1. Preparation of a Key Intermediate" *J. Org. Chem.* **2009**, *74*, 2589–2591.
- Cheung, A. K.; Murelli, R.; Snapper, M. L. "Total Syntheses of (+) and (-)-Cacospongionolide B, Cacospongionolide E, and Related Analogues. Preliminary Study of Structural Features Required for Phospholipase A2 Inhibition" *J. Org. Chem.* **2004**, *69*, 5712–5719.
- Lanfranchi, D. A.; Bour, C.; Hanquet, G. "Enantioselective Access to Key Intermediates for Salvinorin A and Analogues" *Eur. J. Org. Chem.* **2011**, 2818–2826.
- Scheerer, J. R.; Lawrence, J. F.; Wang, G. C.; Evans, D. A. "Asymmetric Synthesis of Salvinorin A, A Potent  $\kappa$  Opioid Receptor Agonist" *J. Am. Chem. Soc.* **2007**, *129*, 8968–8969
- Starr, J. T.; Evans, D. A. "A Cycloaddition Cascade Approach to the Total Synthesis of (-)-FR182877" *J. Am. Chem. Soc.* **2003**, *125*, 13531–13540.

31. Shiina, I.; Mukaiyama, T. "A Novel Method for the Preparation of Macrolides from  $\omega$ -Hydroxycarboxylic Acids". *Chem. Lett.* **1994**, *23*, 677–680.
32. Munro, T. A.; et al. "8-epi-salvinorin B: crystal structure and affinity at the  $\kappa$  opioid receptor". *Beilstein J. Org. Chem.* **2007**, *3*, 1.
33. Nozawa, M.; Suka, Y.; Hoshi, T.; Suzuki, T.; Hagiwara, H. "Total synthesis of the hallucinogenic neoclerodane diterpenoid salvinorin A." *Org. Lett.* **2008**, *10*, 1365–1368.
34. Hagiwara, H.; Hamano, K.; Nozawa, M.; Hoshi, T.; Suzuki, T.; Kido, F. "The First Total Synthesis of (-)-Methyl Barbascoate" *J. Org. Chem.* **2005**, *70*, 2250–2255.
35. Aladro, F. J.; Guerra, F. M.; Moreno-Dorado, F. J.; Bustamante, J. M.; Jorge, Z. D.; Massanet, G. M. "Enantioselective synthesis of (+)-decipienin A" *Tetrahedron* **2001**, *57*, 2171–2178.
36. Hagiwara, H.; Suka, Y.; Nojima, T.; Hoshi, T.; Suzuki, T. "Second-generation synthesis of salvinorin A." *Tetrahedron* **2009**, *65*, 4820–4825.
37. Hagiwara, H.; Nojima, T.; Suka, Y.; Hoshi, T.; Suzuki, T. "First total synthesis of the neo-clerodane diterpenoid salvinorin F" *Nat. Prod. Commun.* **2011**, *6*, 333–335.
38. Line, N. J.; Burns, A. C.; Butler, S. C.; Casbohm, J. Forsyth, C. J. "Total Synthesis of (-)-Salvinorin A." *Chem. Eur. J.* **2016**, *22*, 17983–17986.
39. Wang, Y.; Metz, P. "Total Synthesis of the Neoclerodane Diterpene Salvinorin A via an Intramolecular Diels-Alder Strategy" *Org. Lett.* **2018**, *20*, 3418–3421.
40. Wang, Y.; Rogachev, V.; Wolter, M.; Gruner, M.; Jäger, A.; Metz, P. "An Approach to the Bicyclic C-5-C-17/C-19-C-20 (BC) Portion of Neoclerodane Diterpenes by Intramolecular Diels-Alder Reaction" *Eur. J. Org. Chem.* **2014**, 4083–4088.
41. Hooker, J. M.; Xu, Y.; Schiffer, W.; Shea, C.; Carter, P.; Fowler, J. S. "Pharmacokinetics of the potent hallucinogen, salvinorin A in primates parallels the rapid onset and short duration of effects in humans" *Neuroimage* **2008**, *41*, 1044–1050.
42. MacLean, K. A.; Johnson, M. W.; Reissig, C. J.; Prisinzano, T. E.; Griffiths, R. R. Dose-related effects of salvinorin A in humans: dissociative, hallucinogenic, and memory effects. *Psychopharm. (Berl.)* **2013**, *226*, 381–392.
43. Johnson MW, MacLean KA, Caspers MJ, Prisinzano TE, Griffiths RR. Time course of pharmacokinetic and hormonal effects of inhaled high-dose salvinorin A in humans. *J. Psychopharmacology* **2016**, *30*, 323–329.
44. Prisinzano T. E.; Rothman, R. B. Salvinorin A analogs as probes in opioid pharmacology. *Chem. Rev.* **2008**, *108*, 1732–1743.
45. Kivell, B.M.; Paton, K.F.; Kumar, N.; Morani, A.S.; Culverhouse, A.; Shepherd, A.; Welsh, S. A.; Biggerstaff, A.; Crowley, R. S.; Prisinzano, T. E. *Kappa* Opioid Receptor Agonist Mesyl Sal B Attenuates Behavioral Sensitization to Cocaine with Fewer Aversive Side-Effects than Salvinorin A in Rodents. *Molecules*, **2018**, *23*, 2602.
46. Ewald, A. W. M.; Bosch, P. J.; Culverhouse, A.; Crowley, R. S.; Neuenswander, B.; Prisinzano, T. E.; Kivell, B. M. The C-2 derivatives of salvinorin A, ethoxymethyl ether Sal B and  $\beta$ -tetrahydropyran Sal B, have anti-cocaine properties with minimal side effects. *Psychopharm.* **2017**, *234*, 2499–2514.
47. Sherwood, A. M.; Crowley, R. S.; Paton, K. F.; Biggerstaff, A.; Neuenswander, B.; Day, V. W.; Kivell, B. M.; Prisinzano, T. E. "Addressing Structural Flexibility at the A-Ring on Salvinorin A: Discovery of a Potent Kappa Opioid Agonist with Enhanced Metabolic Stability" *J. Med. Chem.* **2017**, *60*, 3866–3878.
48. Beguin, C.; Richards, M. R.; Li, J. G.; Wang, Y. L.; Xu, W.; Liu-Chen, L. Y.; Carlezon, W. A.; Cohen, B. M. "Synthesis and in vitro evaluation of salvinorin A analogues: Effect of configuration at C(2) and substitution at C(18)" *Bioorg. Med. Chem. Lett.* **2006**, *16*, 4679–4685.
49. Cunningham, C. W.; Rothman, R. B.; Prisinzano, T. E. "Neuropharmacology of the Natural Occurring  $\kappa$ -Opioid Hallucinogen Salvinorin A" *Pharmacol. Rev.* **2011**, *63*, 316–347.
50. Sherwood, A. M.; Williamson, S. E.; Crowley, R. S.; Abbott, L. M.; Day, V. W.; Prisinzano, T. E. "Modular Approach to *pseudo*-Neoclerodanes as Designer  $\kappa$ -Opioid Ligands" *Org. Lett.* **2017**, *19*, 5414–5417.
51. BouzBouz, S.; Cossy, J. "Enantioselective Allyltitanation. Efficient Synthesis of the C1-C4 Polyol Subunit of Amphotericin B" *Org Lett.* **2000**, *2*, 3975–3977.
52. Boeckman R.K.; Biegasiewicz K.F.; Tusch D.J.; Miller J.R. "Organocatalytic Enantioselective  $\alpha$ -Hydroxymethylation of Aldehydes: Mechanistic Aspects and Optimization" *J Org Chem.* **2015**, 4030–4045.
53. Boeckman R.K.; Thomas A. "Methodology for the synthesis of phosphorus-activated tetramic acids: applications to the synthesis of unsaturated 3-acyltetramic acids" *J Org Chem.* **1982**, *47*, 2823–2824.
54. Huffman, T. R.; Wu, Y.; Emmerich, A.; Shenvi, R. A. "Intermolecular Heck Coupling with Hindered Alkenes Directed by Potassium Carboxylates" *Angew. Chem. Int. Ed.* **2019**, *58*, 2371–2376.
55. Engle, K. M.; Mei, T. S.; Wasa, M.; Yu, J. Q. "Weak coordination as a powerful means for developing broadly useful C-H functionalization reactions" *Acc. Chem. Res.* **2012**, *45*, 788–802.
56. Wu, H.; Wacker D.; Katritch, V.; Han, G. W.; Vardy, E.; Liu, W.; Thompson, A. A.; Huang, X. P.; Carroll, F. I.; Mascarella, S. W.; Westkaemper, R. B.; Mosier, P. D.; Roth, B. L.; Cherezov, V.; Stevens, R. C. "Structure of the human  $\kappa$ -opioid receptor in complex with JDTic" *Nature.* **2012**, *485*, 327–332.
57. Hirasawa, S.; Cho, M.; Brust, T. F.; Roach, J. R.; Bohn, L. M.; Shenvi, R. A. "O6C-20-nor-SalA is a stable and potent KOR agonist" *Bioorg. Med. Chem. Lett.* **2018**, *28*, 2770–2772.
58. Böttcher, T. "An Additive Definition of Molecular Complexity" *J. Chem. Inf. Model.* **2016**, *56*, 462–470.
59. Demoret, R. M.; Baker, M. A.; Ohtawa, M.; Chen, S.; Lam, C.-C.; Forli, S.; Houk, K.; Shenvi, R. A. "Synthesis and Mechanistic Interrogation of Ginkgo biloba Chemical Space en route to (-)-Bilobalide" *ChemRxiv* DOI: 10.26434/chemrxiv.12132939.v2
60. Clemons, P. A.; Bodycombe, N. E.; Carrinski, H. A.; Wilson, J. A.; Shamji, A. F.; Wagner, B. K.; Koehler, A. N.; Schreiber, S. L. "Small molecules of different origins have distinct distributions of structural complexity that correlate with protein-binding profiles" *PNAS*, **2010**, *107*, 18787–18792.
61. Schneider, G.; Neidhard W.; Giller, T.; Schmid G. "Scaffold-Hopping" by Topological Pharmacophore Search: A contribution to Virtual Screen" *Angew. Chem. Int. Ed.* **1999**, *38*, 2894–2896.
62. Sun, H.; Tawa, G.; Wallqvist, A. "Classification of scaffold-hopping approaches" *Drug Discovery Today*, **2012**, *17*, 310–324.
63. Houmes, R. J. M.; Voets, M. A.; Verkaaik, A.; Erdmann, W.; Lachmann, B. "Efficacy and Safety of Tramadol Versus Morphine for Moderate and Severe Postoperative Pain With

- Special Regard to Respiratory Depression” *Anesth. Analg.* **1992**, *74*, 510–514.
64. Gupta, A.; Gomes, I.; Bobek, E. N.; Fakira, A. K.; Massaro, N. P.; Sharma, I.; Cavé, A.; Hamm, H. E.; Parelo, J.; Devi, L. A. “Collybolide is a novel biased agonist of  $\kappa$ -opioid receptors with potent antipruritic activity” *Proc. Nat'l. Acad. Sci.* **2016**, *113*, 6041–6046.
65. Váradi, A.; Marrone, G. F.; Palmer, T. C.; Narayan, A.; Szabó, M. R.; Le Rouzic, V.; Grinnell, S. G.; Subrath, J. J.; Warner, E.; Kalra, S.; Hunkele, A.; Pagirsky, J.; Eans, S. O.; Medina, J. M.; Xu, J.; Pan, Y.-X.; Borics, A.; Pasternak, G. W.; McLaughlin, J. P.; Majumdar, S. “Mitragynine/Corynantheidine Pseudoindoxyls As Opioid Analgesics with Mu Agonism and Delta Antagonism, Which Do Not Recruit  $\beta$ -Arrestin-2” *J. Med. Chem.* **2016**, *59*, 8381–8397.
66. Tsujikawa, K.; Kuwayama, K.; Miyaguchi, H.; Kanamori T.; Iwata, Y. T.; Inoue, H. “*In Vitro* stability and metabolism of salvinorin A in rat plasma” *Xenobiotica*, **2009**, *39*, 391–398.
67. Fishbane, S.; Jamal, A.; Munera, C.; Wen, W.; Menzaghi, F. “A Phase 3 Trial of Difelikefalin in Hemodialysis Patients with Pruritus” *N. Engl. J. Med.* **2020**, *382*, 222–232.
68. Burch, R. L.; Atkinson, T. J. “Inside the Potential of Peripheral Kappa Opioid Receptor Agonists” *Pract. Pain Manag.* **2020**, *20*, 23–27.
69. Trauner, D.; Schoenberger, M. “A Photochromic Agonist for  $\mu$ -Opioid Receptors” *Angew. Chem. Int. Ed.* **2014**, *53*, 3264–3267
70. Kane, B. E.; Nieto, M. J.; McCurdy, C. R.; Ferguson, D. M. “A unique binding epitope for salvinorin A, a non-nitrogenous kappa opioid receptor agonist” *FEBS J.* **2006**, *273*, 1966–1974.

## TOC GRAPHIC

